Nuclear structure aspects of nuclear matrix elements in neutrinoless double-beta decay

Tomás R. Rodríguez

XIIIth Quark Confinement and the Hadron Spectrum 2018

Maynooth 05/08/2018

Acknowledgments

G. Martínez-Pinedo (GSI/TU-Darmstadt)

J. Menéndez (University of Tokyo)

N. López-Vaquero (UAM-Madrid)

J. L. Egido (UAM-Madrid)

A. Poves (UAM-Madrid)

J. Engel (UNC-Chapel Hill)

N. Hinohara (University of Tsukuba)

1. Introduction

2. Deformation

3. Pairing (nn, pp, pn)

4. Other nuclear structure effects

5. Summary

Double beta decay

Process mediated by the weak interaction which occurs in those even-even nuclei where the single beta decay is energetically forbidden.

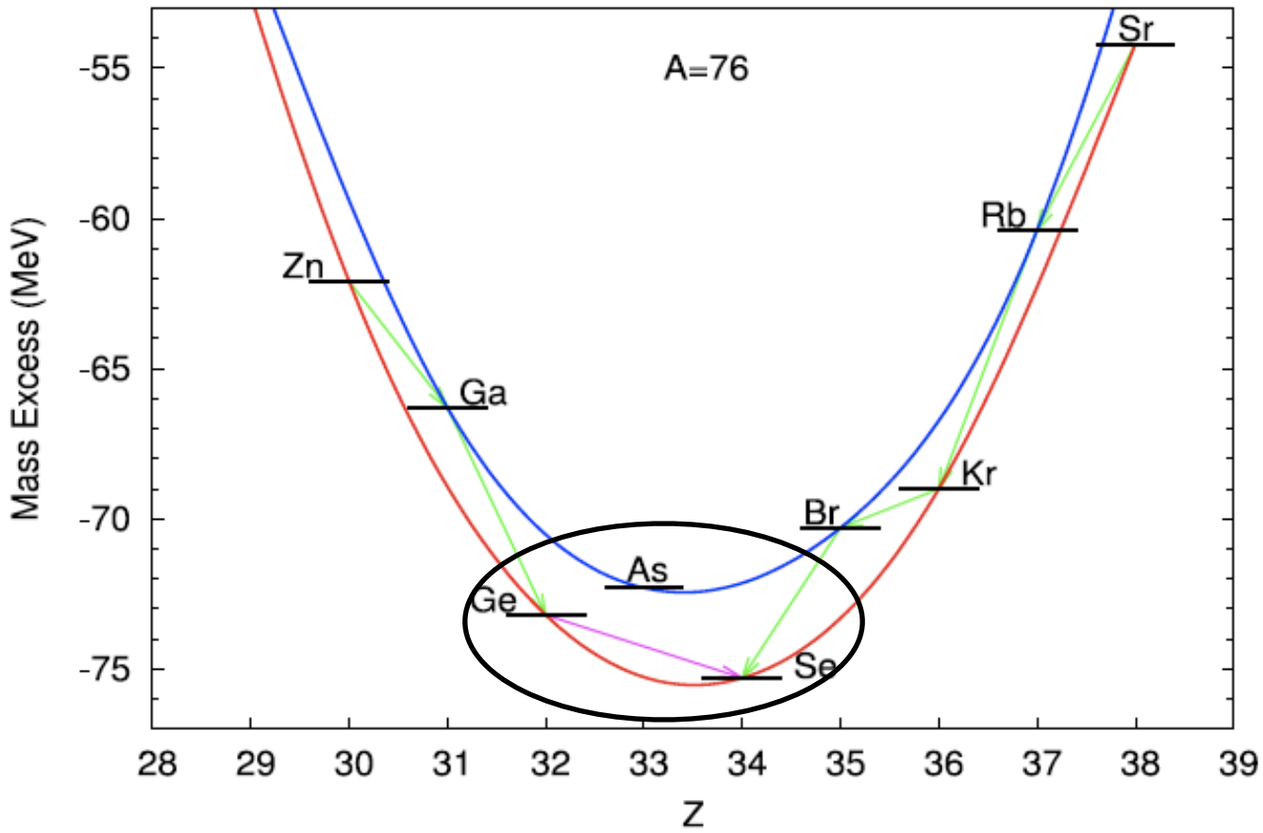

Double beta decay

Process mediated by the weak interaction which occurs in those even-even nuclei w decay is energetically forb

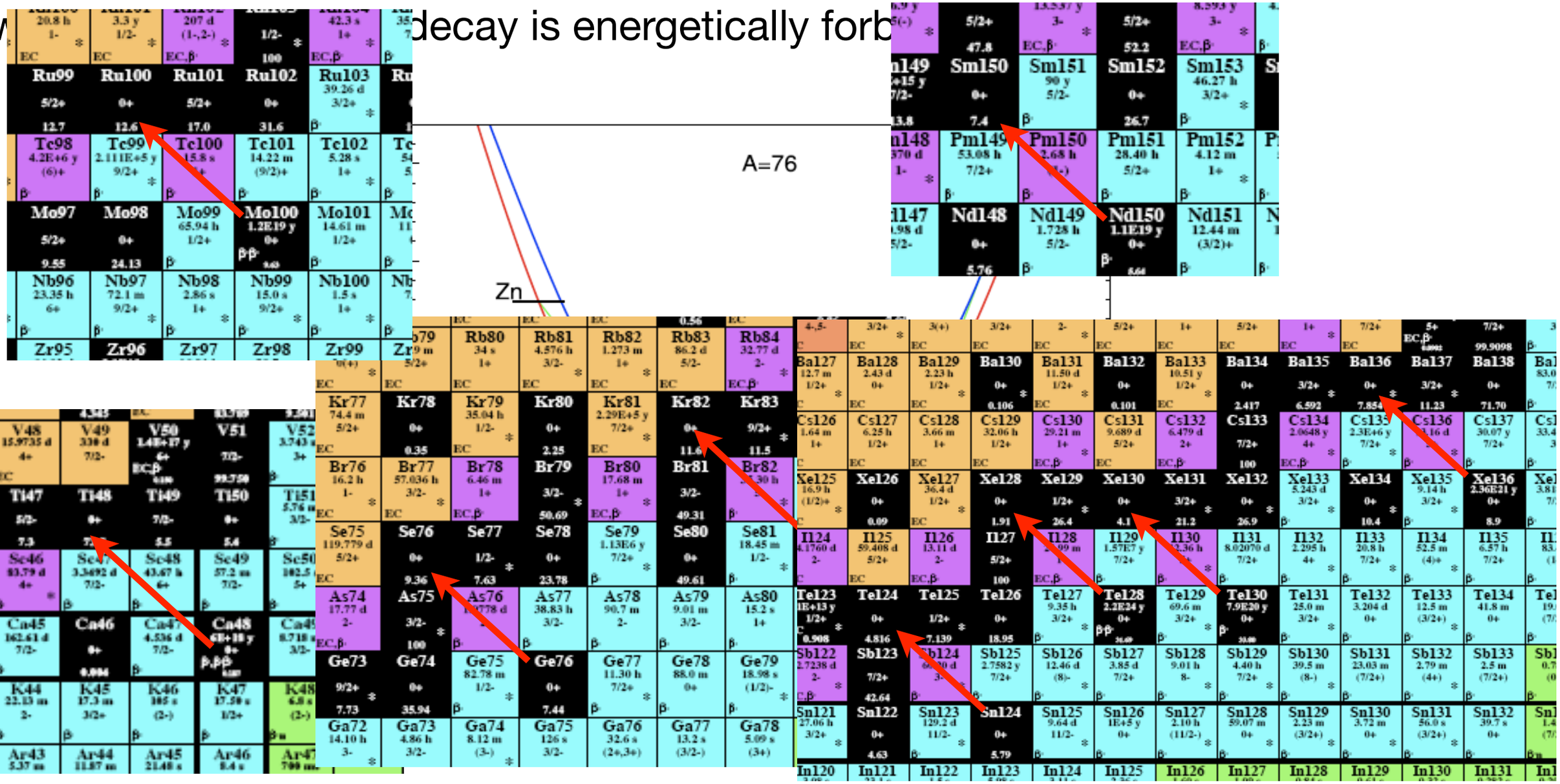

Double beta decay

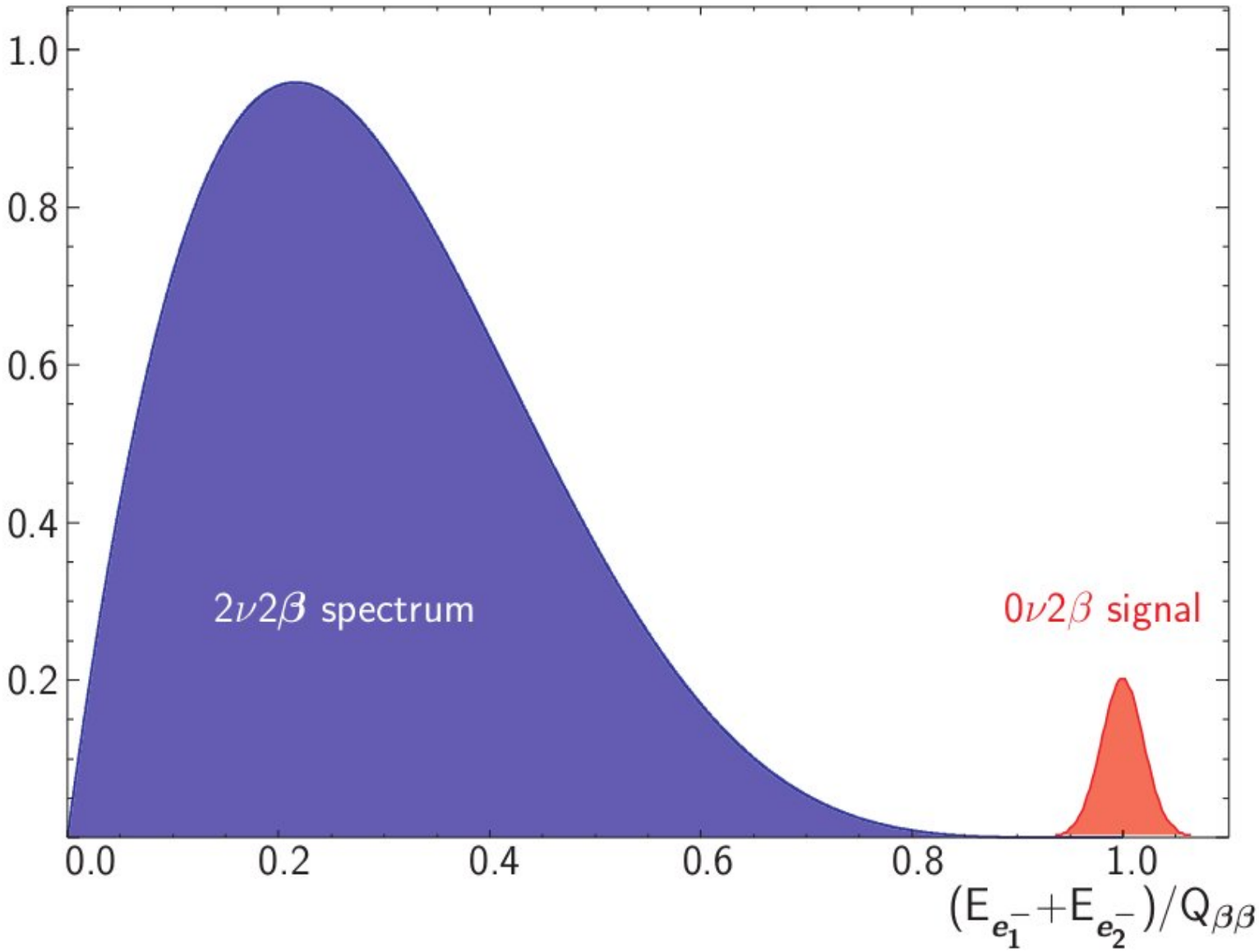

Only lower limits to the half-lives have been measured so far

Double beta decay

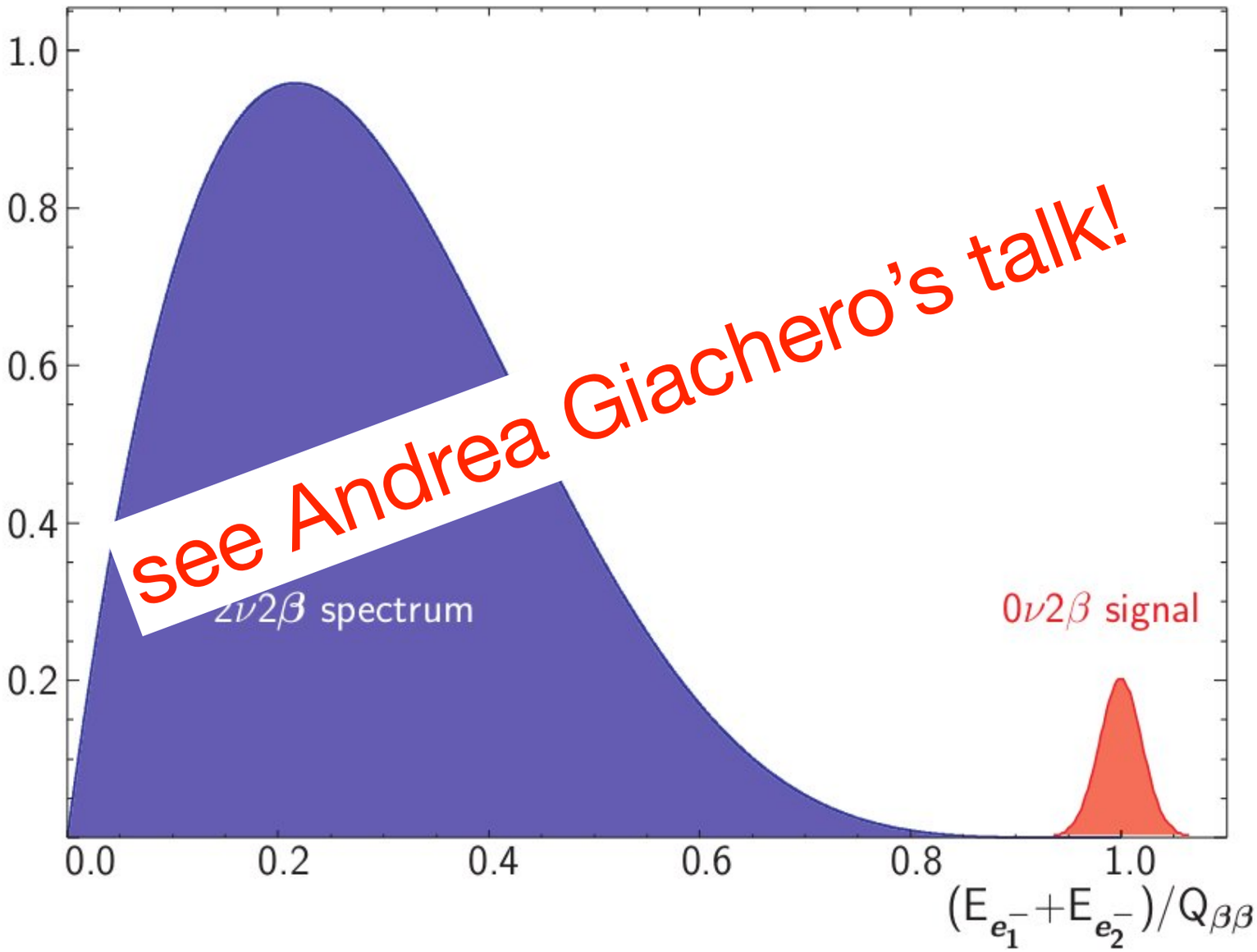

see Andrea Giachero's talk!

Only lower limits to the half-lives have been measured so far

Neutrinoless double beta decay

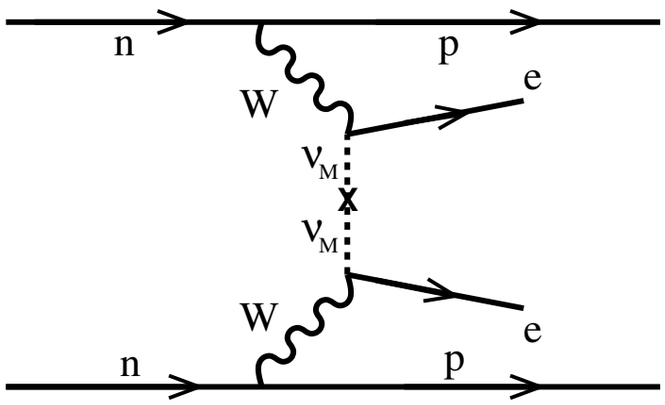

$$ {}^{A}_{Z}X_N \rightarrow {}^{A}_{Z+2}Y_{N-2} + 2e^- $$

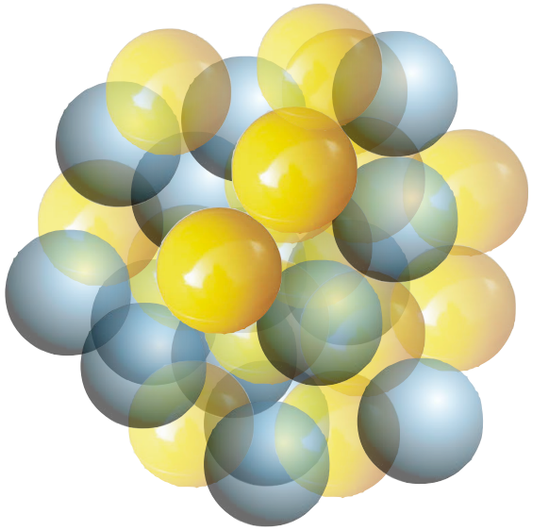

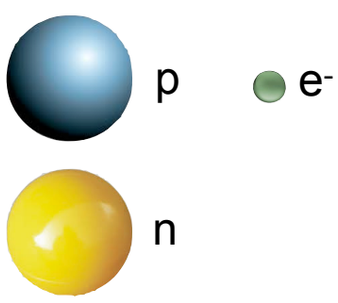

Neutrinoless double beta decay

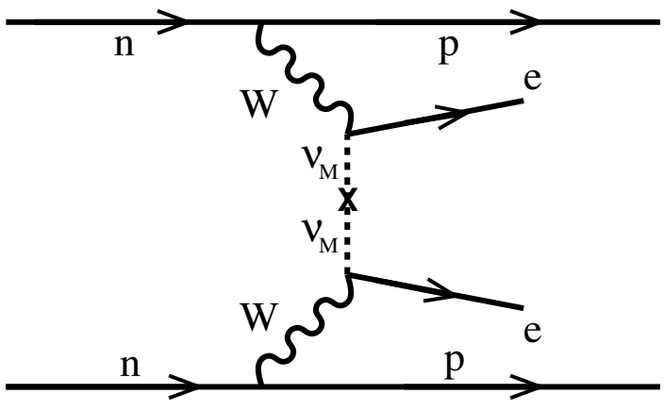

$$ {}^{A}_{Z}X_N \rightarrow {}^{A}_{Z+2}Y_{N-2} + 2e^- $$

- Violates the leptonic number conservation
- Neutrinos are massive Majorana particles
- Mass hierarchy of neutrinos
- Experimentally not observed ($T_{1/2} > 10^{25}$ y)
- Beyond the Standard Model
- Most plausible mechanism: exchange of light Majorana neutrinos

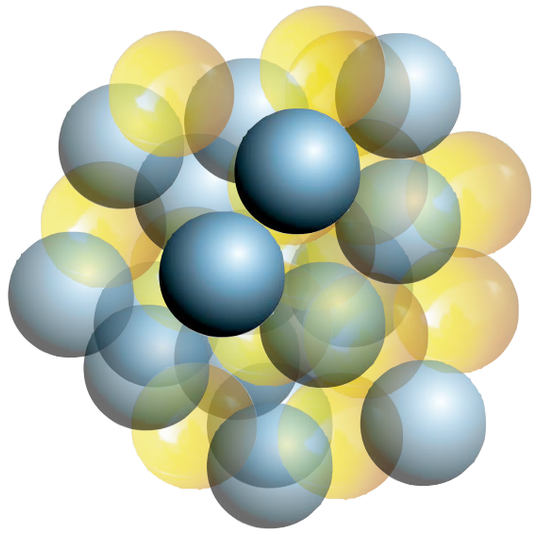

p e^-

n

Neutrinoless double beta decay

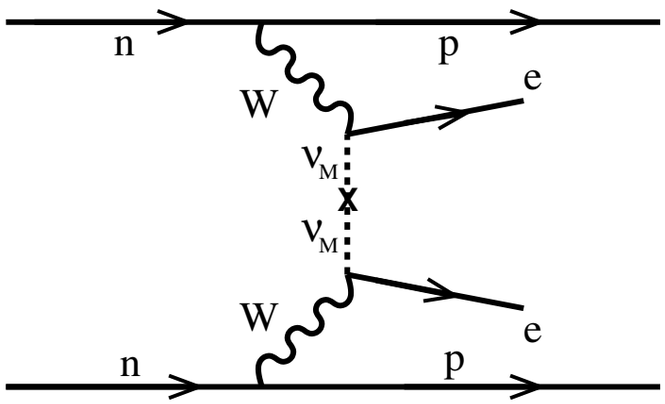

$$ {}^{A}_{Z}X_N \rightarrow {}^{A}_{Z+2}Y_{N-2} + 2e^- $$

- Violates the leptonic number conservation
- Neutrinos are massive Majorana particles
- Mass hierarchy of neutrinos
- Experimentally not observed ($T_{1/2} > 10^{25}$ y)
- Beyond the Standard Model
- Most plausible mechanism: exchange of light Majorana neutrinos

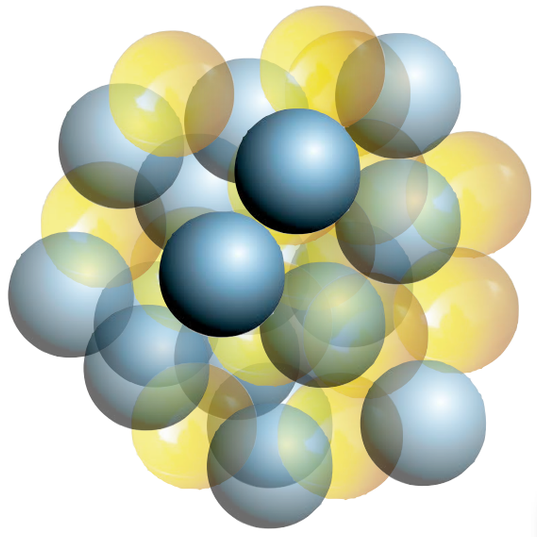

p e- n

$$ \left(T^{0\nu\beta\beta}_{1/2}(0^+ \rightarrow 0^+) \right)^{-1} = G_{01} \left| M^{0\nu\beta\beta} \right|^2 \left(\frac{\langle m_{\beta\beta} \rangle}{m_e} \right)^2 $$

Neutrinoless double beta decay

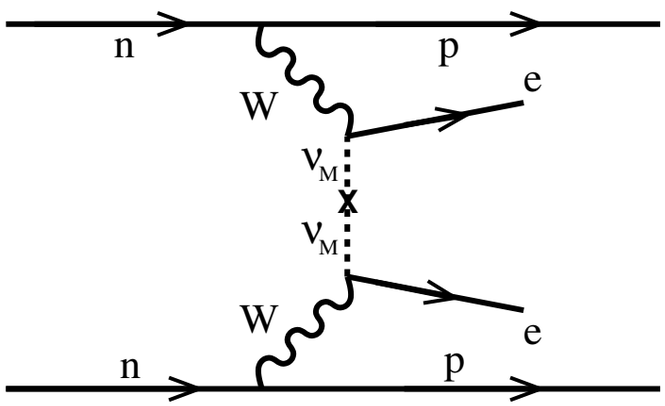

$$ {}^{A}_{Z}X_N \rightarrow {}^{A}_{Z+2}Y_{N-2} + 2e^- $$

- Violates the leptonic number conservation
- Neutrinos are massive Majorana particles
- Mass hierarchy of neutrinos
- Experimentally not observed ($T_{1/2} > 10^{25}$ y)
- Beyond the Standard Model
- Most plausible mechanism: exchange of light Majorana neutrinos

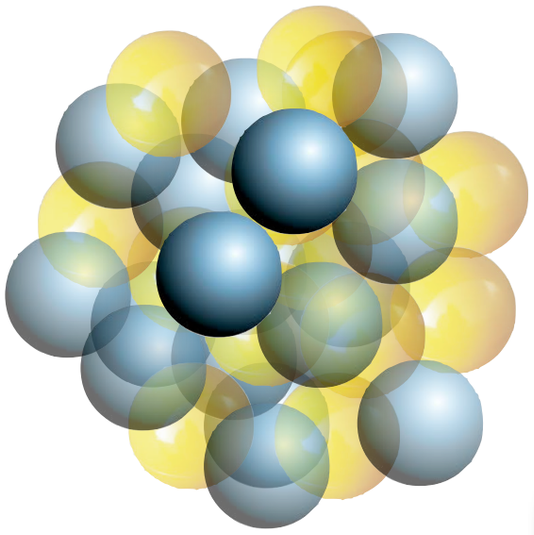

p e⁻ n

$$ \left(T^{0\nu\beta\beta}_{1/2}(0^+ \rightarrow 0^+)\right)^{-1} = G_{01} \left|M^{0\nu\beta\beta}\right|^2 \left(\frac{\langle m_{\beta\beta}\rangle}{m_e}\right)^2 $$

Phys. Rev. C 85, 034316 (2012).

Phys. Rev. C 88, 037303 (2013).

Phase space factor

Neutrinoless double beta decay

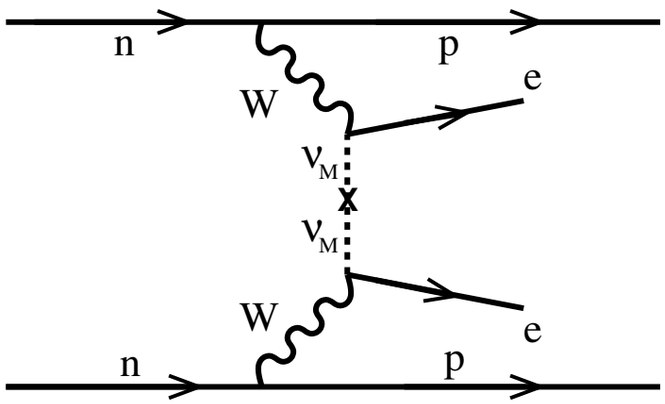

$$ {}^{A}_{Z}X_N \rightarrow {}^{A}_{Z+2}Y_{N-2} + 2e^- $$

- Violates the leptonic number conservation
- Neutrinos are massive Majorana particles
- Mass hierarchy of neutrinos
- Experimentally not observed ($T_{1/2} > 10^{25}$ y)
- Beyond the Standard Model
- Most plausible mechanism: exchange of light Majorana neutrinos

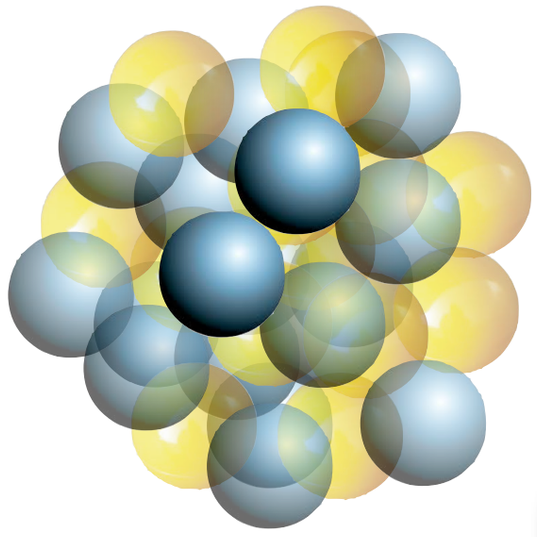

p e- n

$$ \left(T^{0\nu\beta\beta}_{1/2}(0^+ \rightarrow 0^+)\right)^{-1} = G_{01} \left|M^{0\nu\beta\beta}\right|^2 \left(\frac{\langle m_{\beta\beta}\rangle}{m_e}\right)^2 $$

Nuclear Matrix Element

NME: Starting points

- Leading lepton number violating process contributing to 0νββ decay
  - **Exchange of light Majorana neutrino.**
  - Exchange of heavy Majorana neutrino.
  - Leptoquarks.
  - Supersymmetric particles.
  - ...
- Transition operator connecting initial and final states
  - Relativistic/Non-relativistic.
  - Nucleon size effects.
  - Two-body weak currents.
  - Short-range correlations.
  - Closure approximation.
  - ...

- Nuclear structure method (fully consistent or not with the operator) for calculating these NME.
  - Correlations.
  - Symmetry conservation.
  - Valence space.
  - ...

NME: Starting points

- Leading lepton number violating process contributing to 0νββ decay
  - **Exchange of light Majorana neutrino.**
  - Exchange of heavy Majorana neutrino.
  - Leptoquarks.
  - Supersymmetric particles.
  - ...
- Transition operator connecting initial and final states
  - Relativistic/Non-relativistic.
  - Nucleon size effects.
  - Two-body weak currents.
  - Short-range correlations.
  - Closure approximation.
  - ...

- Nuclear structure method (fully consistent or not with the operator) for calculating these NME.
  - Correlations.
  - Symmetry conservation.
  - Valence space.
  - ...

NME: Starting points

$$M^{0\nu\beta\beta} = -\left(\frac{g_V(0)}{g_A(0)}\right)^2 M_F^{0\nu\beta\beta} + M_{GT}^{0\nu\beta\beta} - M_T^{0\nu\beta\beta}$$

- Each term can be written as the expectation value of a transition operator acting on the initial al final states:

$$M_\xi^{0\nu\beta\beta} = \langle 0_f^+ | \hat{O}_\xi^{0\nu\beta\beta} | 0_i^+ \rangle$$

- Nuclear structure methods for calculating these NME deal with:

  - Finding the best initial and final ground states.

  - Handling the transition operator (inclusion of most relevant terms, corrections, approximations, etc.).

Nuclear structure methods

Method	Some recent (and key) references
Interacting Shell Model (ISM)	- Phys. Rev. Lett. 100, 052503 (2008). - Nucl. Phys. A 818, 139 (2009). - Phys. Rev. C 87, 014320 (2013). - Phys. Rev. Lett. 113, 262501 (2014). - Phys. Rev. Lett. 116, 112502 (2016).
pnQRPA	- Phys. Rev. C 77, 045503 (2008). - Phys Rev. C 87, 045501 (2013). - J. Phys. G 39, 124005 (2012).
Interacting Boson Model (IBM)	- Phys. Rev. C 79, 044301 (2009). - Phys Rev. C 87, 014315 (2013). - Phys. Rev. C 96, 064305 (2017).
Generator Coordinate Method (GCM-EDF)	- Phys. Rev. Lett. 105, 252503 (2010). - Phys. Rev. Lett 111, 142501 (2013). - Phys. Rev. C 90, 031031(R) (2014). - Phys. Rev. C 90, 054309 (2014). - Phys. Rev. C 91, 024316 (2015). - Phys. Rev. C 96, 054310 (2017). - arXiv:1709.05313 - arXiv:1807.11053

Nuclear structure methods

Method	Some recent (and key) references
Interacting Shell Model (ISM)	- Phys. Rev. Lett. 100, 052503 (2008). - Nucl. Phys. A 818, 139 (2009). - Phys. Rev. C 87, 014320 (2013). - Phys. Rev. Lett. 113, 262501 (201[illegible] - Phys. Rev. Lett. 116, 11[illegible]
pnQRPA	- Phys. Rev. C [illegible] (2009). C 87, 014315 (2013). Phys. Rev. C 96, 064305 (2017).
Interacting Bo[illegible]	
Generator Coordinate Method (GCM-EDF)	- Phys. Rev. Lett. 105, 252503 (2010). - Phys. Rev. Lett 111, 142501 (2013). - Phys. Rev. C 90, 031031(R) (2014). - Phys. Rev. C 90, 054309 (2014). - Phys. Rev. C 91, 024316 (2015). - Phys. Rev. C 96, 054310 (2017). - arXiv:1709.05313 - arXiv:1807.11053

see Amy Nicholson's talk tomorrow for lattice QCD calculations!

Current theoretical status

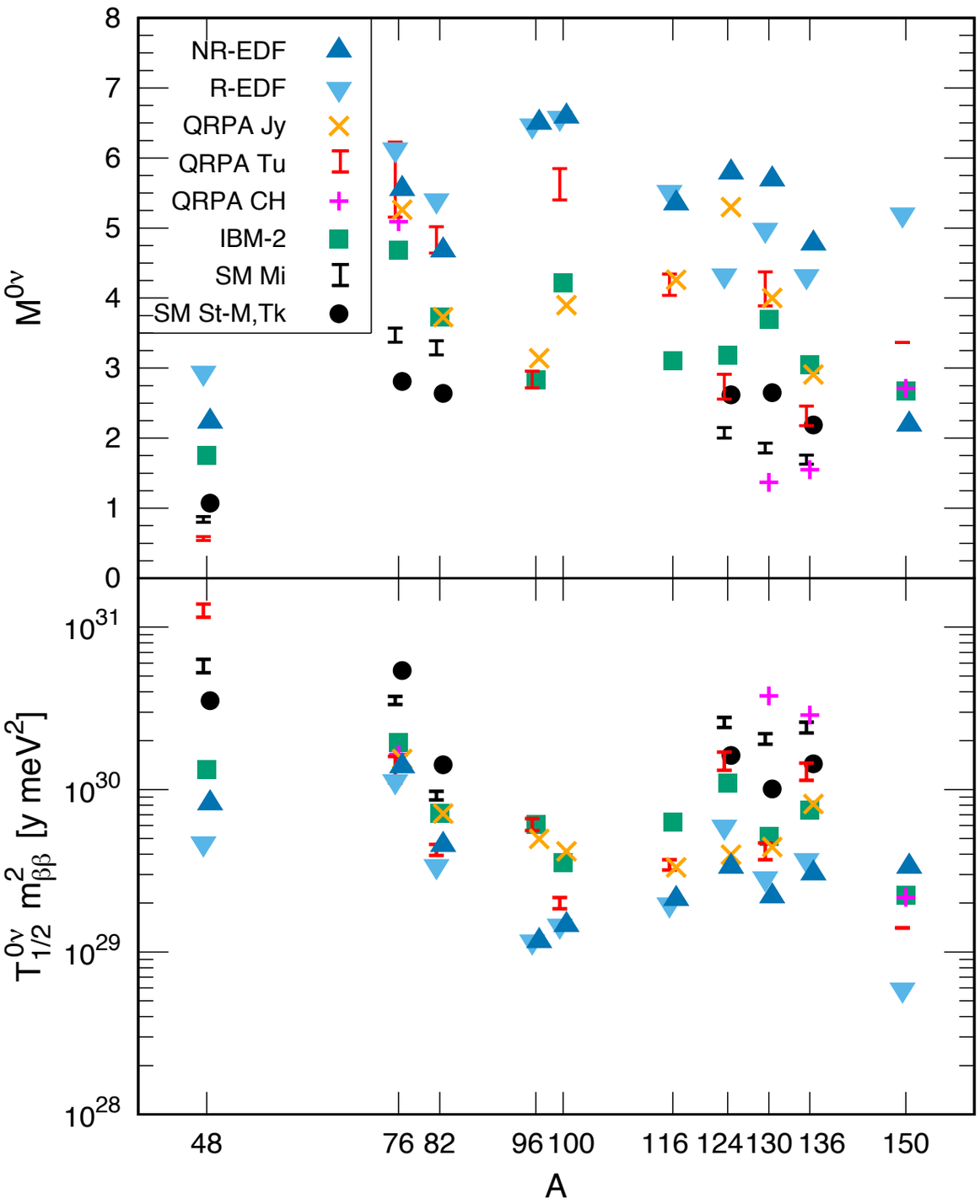

Different methods give different values of NME's with a factor ~3 difference

J. Engel and J. Menéndez, Reports on Progress in Physics 80, 046301 (2017)

Current theoretical status

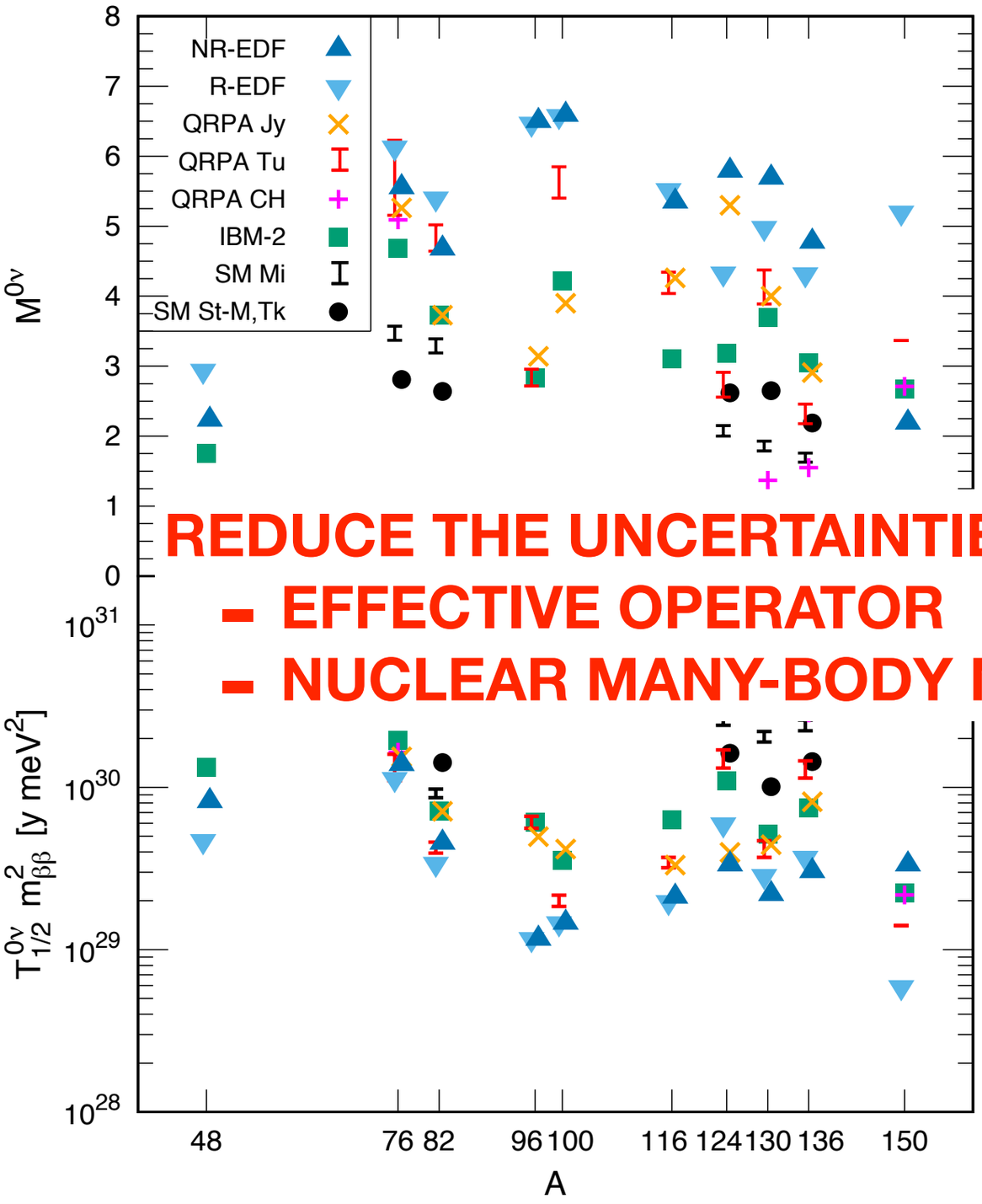

Different methods give different values of NME's with a factor ~3 difference

REDUCE THE UNCERTAINTIES:

- **EFFECTIVE OPERATOR**
- **NUCLEAR MANY-BODY METHOD (CORRELATIONS)**

J. Engel and J. Menéndez, Reports on Progress in Physics 80, 046301 (2017)

NME: Nuclear structure aspects

We want to study the role of

- Deformation and shape mixing.
- Pairing pp/nn/pn correlations.
- Shell effects.
- Isospin conservation.
- Pair breaking (seniority).
- Occupation numbers.
- Size of the valence space.

in the nuclear matrix elements using a standard prescription for the transition operator.

Many-body methods in nuclear structure

SELF-CONSISTENT MEAN-FIELD AND BEYOND-MEAN-FIELD

- Variational approach with simple trial wave functions (HFB) using ‘universal’ functionals.
- Parameters of the functional fitted to bulk properties and masses and radii of finite nuclei.
- Applicable to the whole nuclear chart (0νββ, r-process nucleosynthesis, ...).
- Very precise description of ground state properties and collective phenomena.
- Spectroscopy and nuclear response with beyond mean-field techniques (GCM, QRPA, ...)

LARGE SCALE SHELL MODEL

- Exact diagonalizations within a valence space.
- Effective interactions adapted to the valence space and adjusted to reproduce the evolution of single particle energies (monopoles).
- Very precise description of spectroscopy and transitions of nuclei.
- Limited by the combinatorial increase of the number of configurations.

Many-body methods in nuclear structure

SELF-CONSISTENT MEAN-FIELD AND BEYOND-MEAN-FIELD

- Variational approach with simple trial wave functions (HFB) using 'universal' functionals.
- Parameters of the functional fitted to bulk properties and masses and radii of finite nuclei.
- Applicable to the whole nuclear chart (0νββ, r-process nucleosynthesis, ...).
- Very precise description of ground state properties and collective phenomena.
- Spectroscopy and nuclear response with beyond mean-field techniques (GCM, QRPA, ...)

LARGE SCALE SHELL MODEL

- Exact diagonalizations within a valence spac
- Effective interactions adapted to th
space and adjusted to re
single particle
- Ve
copy and
combinatorial increase of the
nu
er of configurations.

see Philipp Klos' talk on Thursday!

Generator Coordinate Method (GCM)

Determination of initial and final states (I)

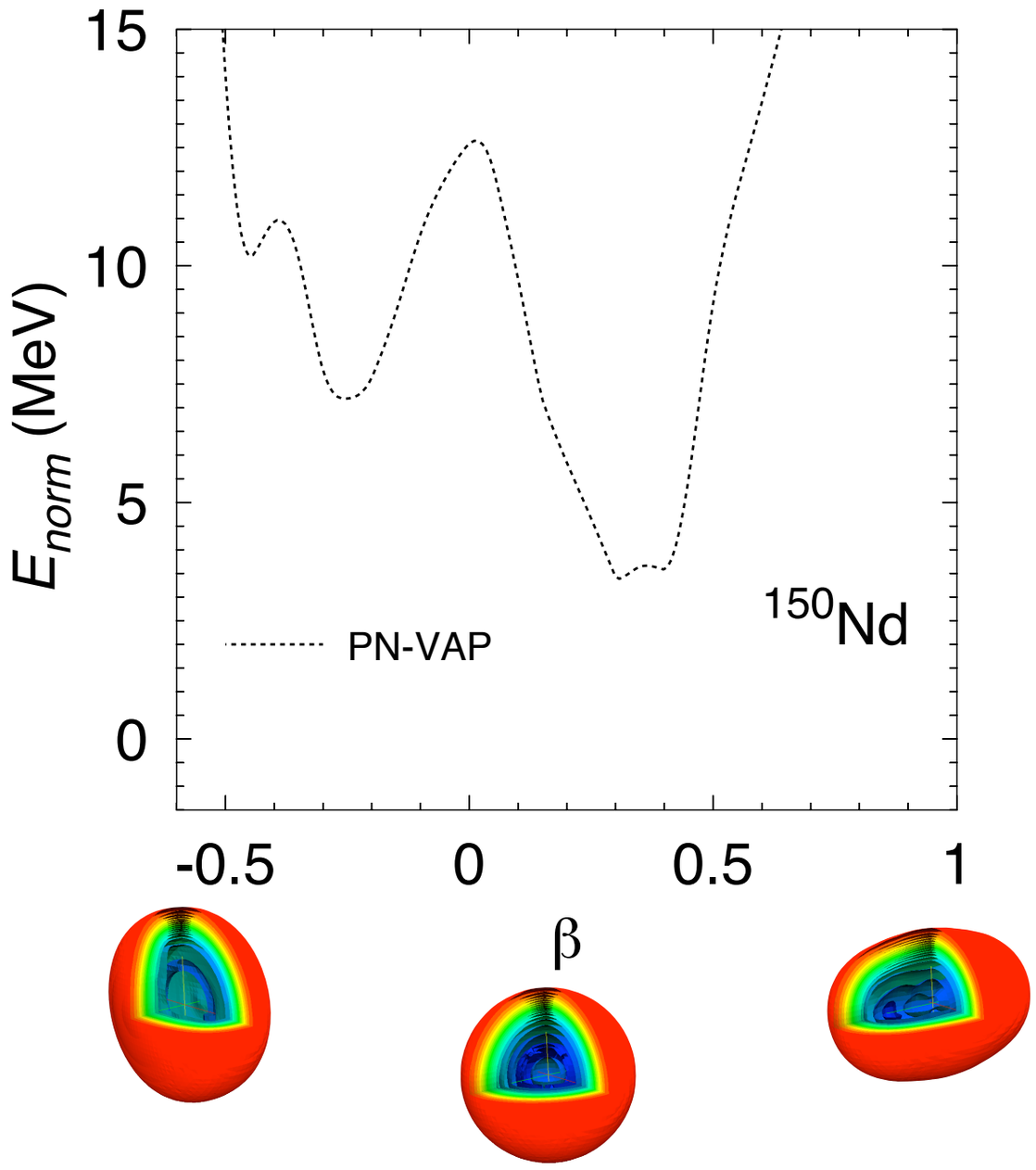

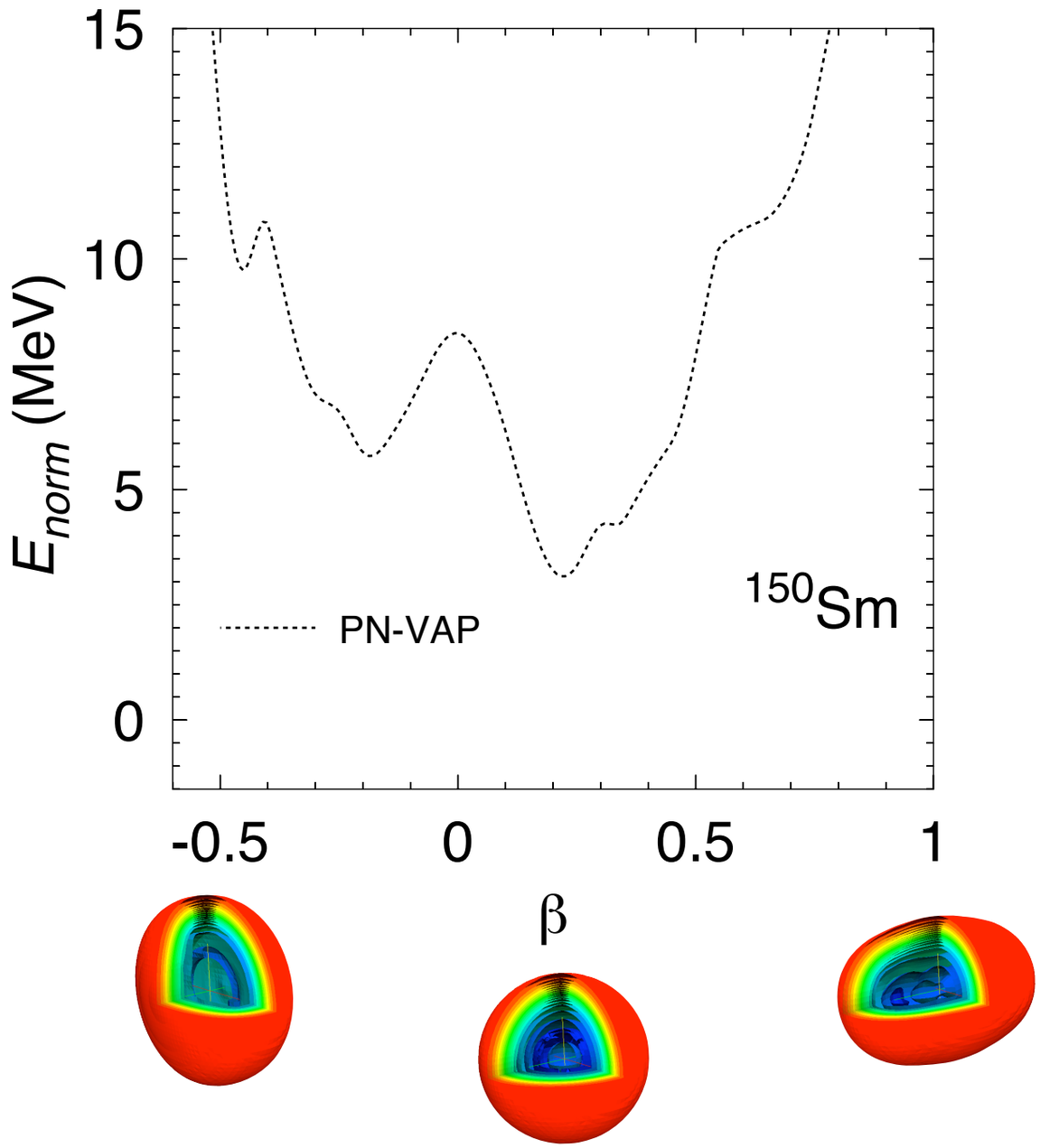

Generator Coordinate Method (GCM)

Determination of initial and final states (II)

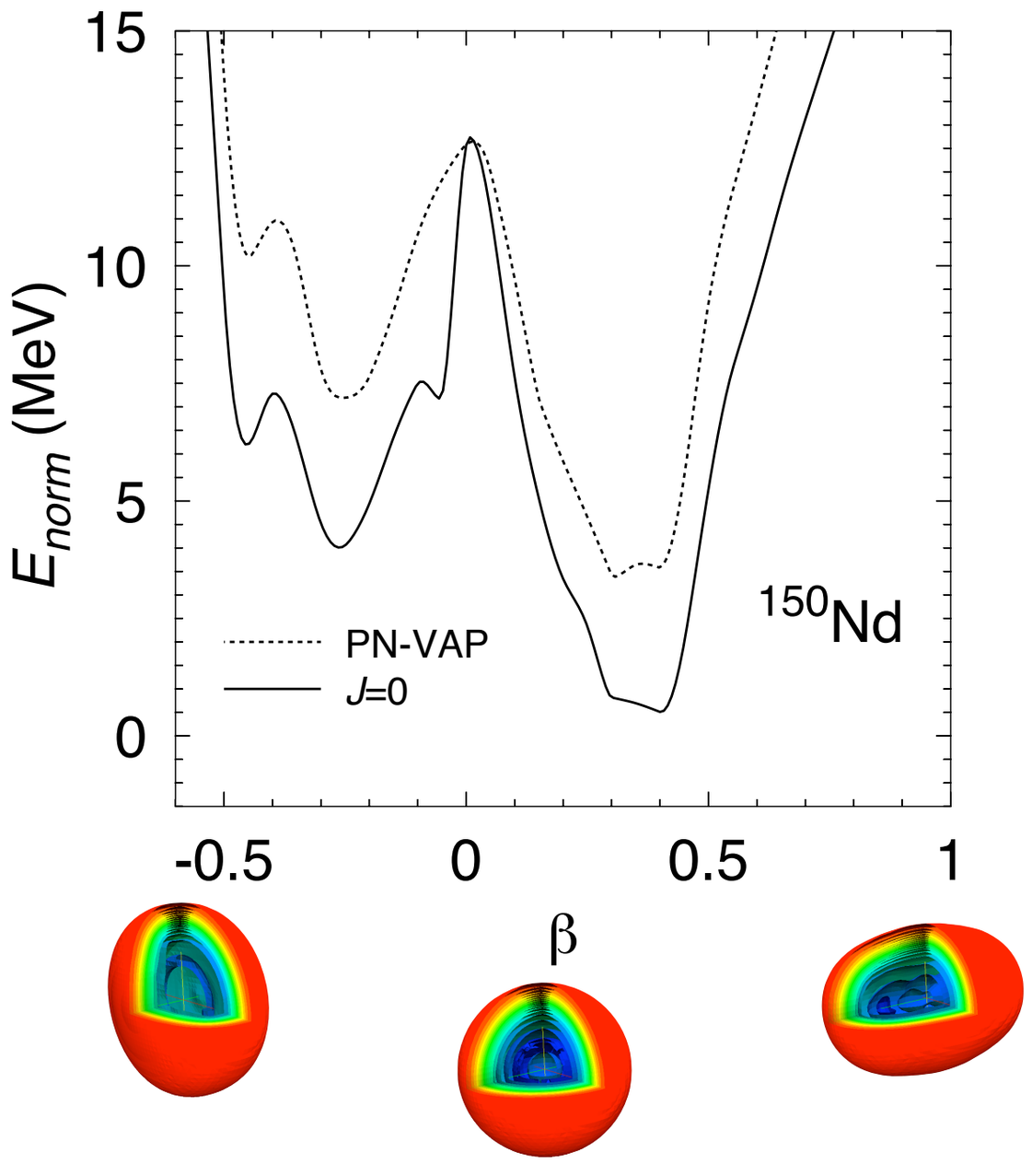

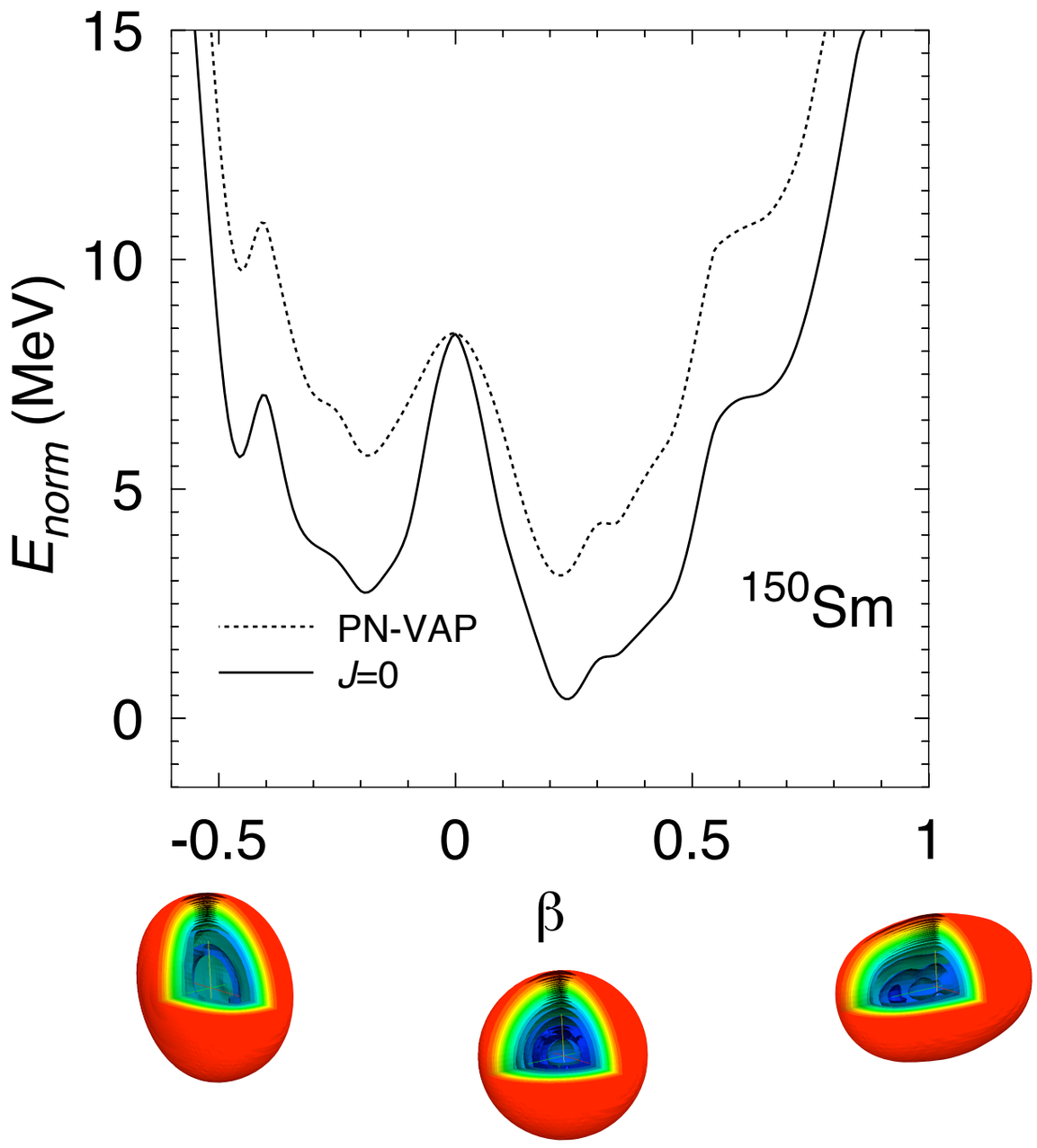

Generator Coordinate Method (GCM)

Determination of initial and final states (& III)

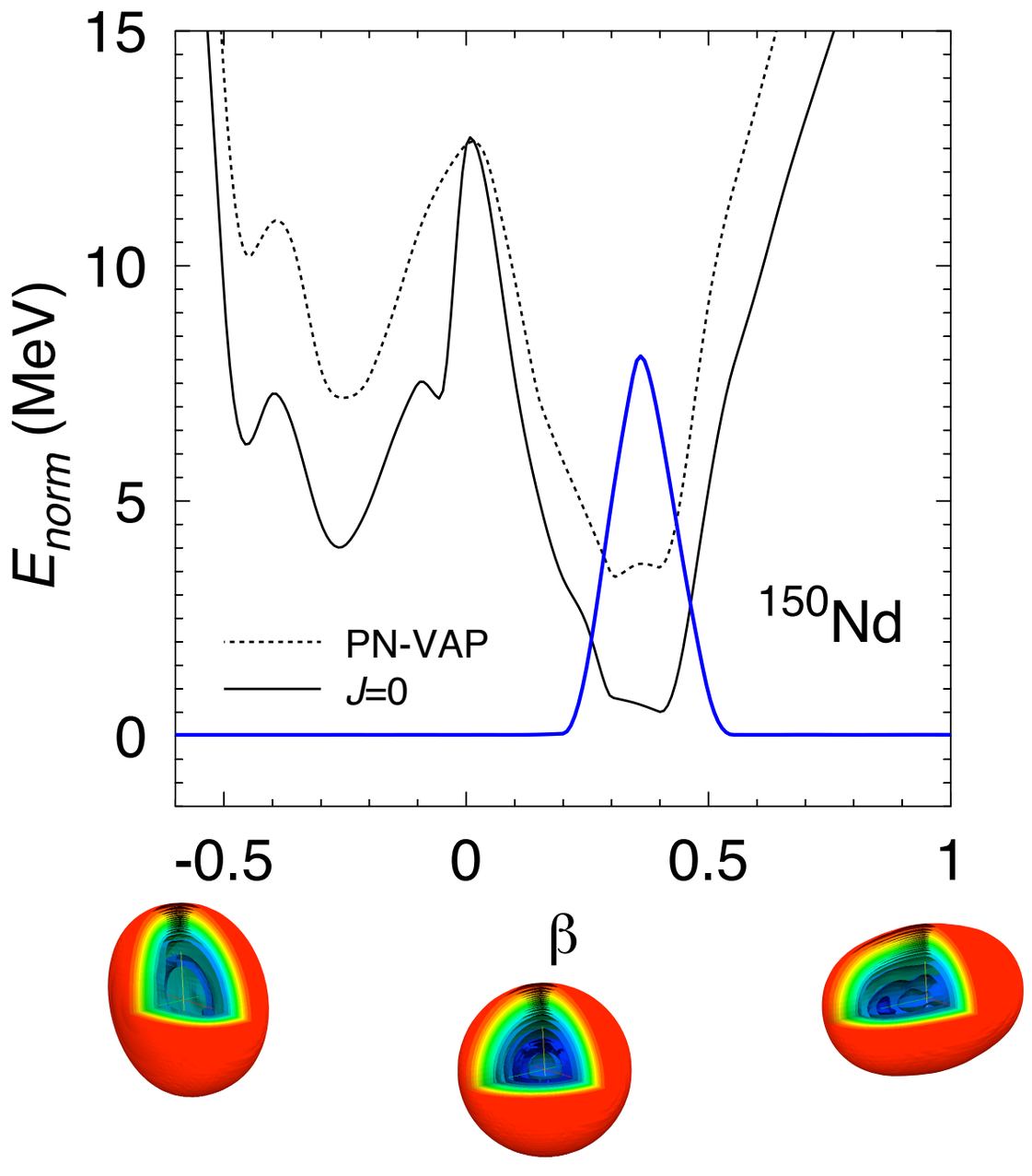

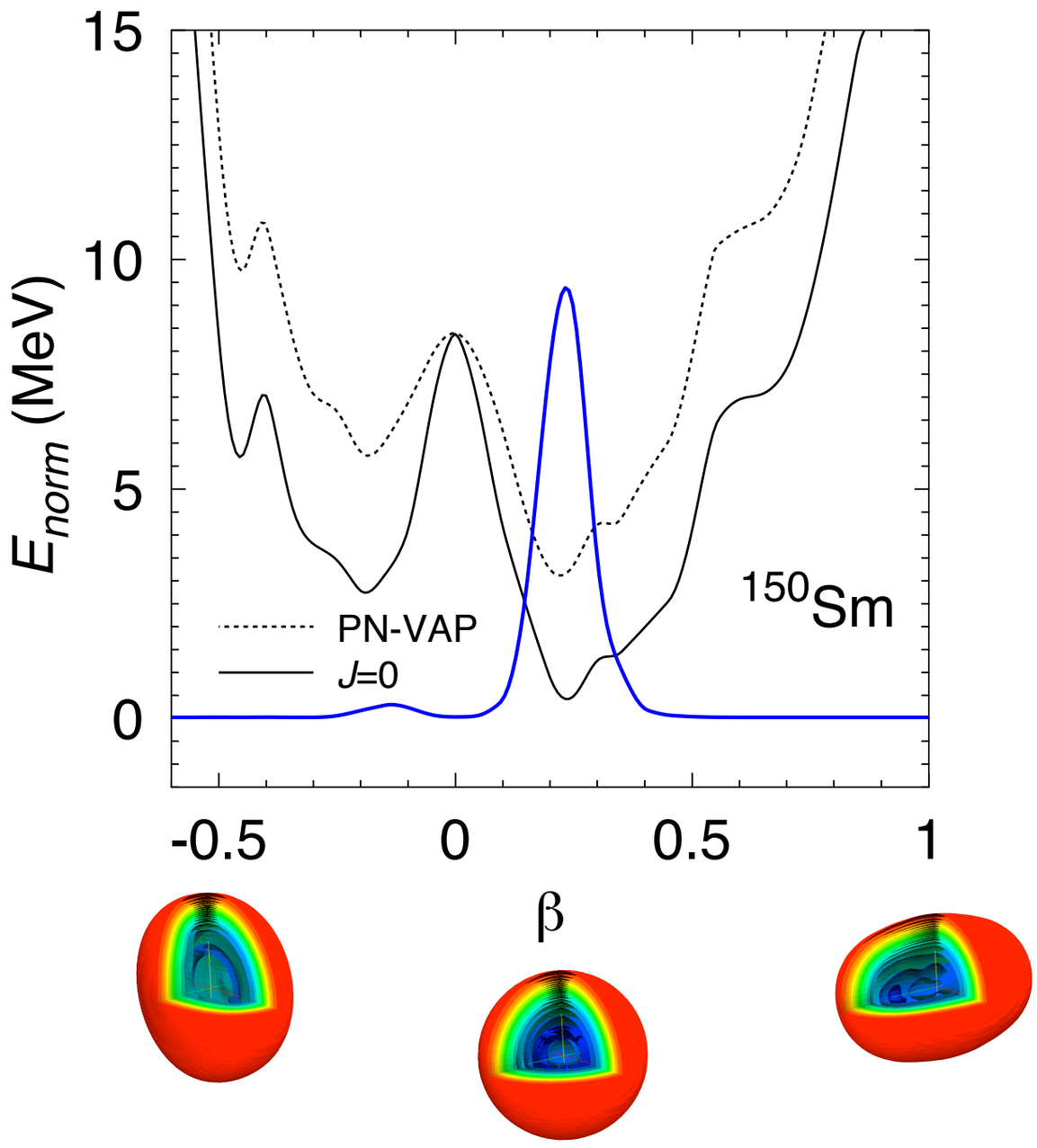

Transitions

1. Angular momentum $I = 0$
2. Axial quadrupole deformations $q = q_{20}$
3. Axial+triaxial quadrupole deformations $q = (q_{20}, q_{22})$
3. Quadrupole and pairing pp/nn correlations $q = (q_{20}, \delta)$
4. Quadrupole and pn correlations $q = (q_{20}, p_0)$
5. Quadrupole and octupole deformations $q = (q_{20}, q_{30})$

$$|0; N_i Z_i; \sigma\rangle = \sum_{\Lambda_i} G^{0;N_i Z_i;\sigma}_{\Lambda_i} |\Lambda^{0;N_i Z_i}_i\rangle$$

$$|0; N_f Z_f; \sigma\rangle = \sum_{\Lambda_f} G^{0;N_f Z_f;\sigma}_{\Lambda_f} |\Lambda^{0;N_f Z_f}_f\rangle$$

Transitions

1. Angular momentum $I = 0$
2. Axial quadrupole deformations $q = q_{20}$
3. Axial+triaxial quadrupole deformations $q = (q_{20}, q_{22})$
3. Quadrupole and pairing pp/nn correlations $q = (q_{20}, \delta)$
4. Quadrupole and pn correlations $q = (q_{20}, p_0)$
5. Quadrupole and octupole deformations $q = (q_{20}, q_{30})$

$$\longrightarrow$$

$$|0; N_i Z_i; \sigma\rangle = \sum_{\Lambda_i} G^{0;N_i Z_i;\sigma}_{\Lambda_i} |\Lambda_i^{0;N_i Z_i}\rangle$$

$$|0; N_f Z_f; \sigma\rangle = \sum_{\Lambda_f} G^{0;N_f Z_f;\sigma}_{\Lambda_f} |\Lambda_f^{0;N_f Z_f}\rangle$$

TRANSITIONS:

$$M^{0\nu\beta\beta}_{\xi} = \langle 0^+_f | \hat{O}^{0\nu\beta\beta}_{\xi} | 0^+_i \rangle = \langle 0; N_f Z_f | \hat{O}^{0\nu\beta\beta}_{\xi} | 0; N_i Z_i \rangle =$$

$$\sum_{\Lambda_f \Lambda_i} \left(G^{0;N_f Z_f}_{\Lambda_f} \right)^* \langle \Lambda_f^{0;N_f Z_f} | \hat{O}^{0\nu\beta\beta}_{\xi} | \Lambda_i^{0;N_i Z_i} \rangle G^{0;N_i Z_i}_{\Lambda_i} = \sum_{q_i q_f ; \Lambda_f \Lambda_i}$$

$$\left(\frac{u^{0;N_f Z_f}_{q_f, \Lambda_f}}{\sqrt{n^{0;N_f Z_f}_{\Lambda_f}}} \right)^* \left(G^{0;N_f Z_f}_{\Lambda_f} \right)^* \langle 0; N_f Z_f; q_f | \hat{O}^{0\nu\beta\beta}_{\xi} | 0; N_i Z_i; q_i \rangle \left(G^{0;N_i Z_i}_{\Lambda_i} \right) \left(\frac{u^{0;N_i Z_i}_{q_i, \Lambda_i}}{\sqrt{n^{0;N_i Z_i}_{\Lambda_i}}} \right)$$

Transitions

1. Angular momentum $I = 0$
2. Axial quadrupole deformations $q = q_{20}$
3. Axial+triaxial quadrupole deformations $q = (q_{20}, q_{22})$
3. Quadrupole and pairing pp/nn correlations $q = (q_{20}, \delta)$
4. Quadrupole and pn correlations $q = (q_{20}, p_0)$
5. Quadrupole and octupole deformations $q = (q_{20}, q_{30})$

$$|0; N_i Z_i; \sigma\rangle = \sum_{\Lambda_i} G^{0;N_i Z_i;\sigma}_{\Lambda_i} |\Lambda^{0;N_i Z_i}_i\rangle$$

$$|0; N_f Z_f; \sigma\rangle = \sum_{\Lambda_f} G^{0;N_f Z_f;\sigma}_{\Lambda_f} |\Lambda^{0;N_f Z_f}_f\rangle$$

TRANSITIONS:

$$M^{0\nu\beta\beta}_\xi = \langle 0^+_f | \hat{O}^{0\nu\beta\beta}_\xi | 0^+_i \rangle = \langle 0; N_f Z_f | \hat{O}^{0\nu\beta\beta}_\xi | 0; N_i Z_i \rangle =$$

$$\sum_{\Lambda_f \Lambda_i} \left(G^{0;N_f Z_f}_{\Lambda_f} \right)^* \langle \Lambda^{0;N_f Z_f}_f | \hat{O}^{0\nu\beta\beta}_\xi | \Lambda^{0;N_i Z_i}_i \rangle G^{0;N_i Z_i}_{\Lambda_i} = \sum_{q_i q_f ; \Lambda_f \Lambda_i}$$

$$\left(\frac{u^{0;N_f Z_f}_{q_f,\Lambda_f}}{\sqrt{n^{0;N_f Z_f}_{\Lambda_f}}} \right)^* \left(G^{0;N_f Z_f}_{\Lambda_f} \right)^* \langle 0; N_f Z_f; q_f | \hat{O}^{0\nu\beta\beta}_\xi | 0; N_i Z_i; q_i \rangle \left(G^{0;N_i Z_i}_{\Lambda_i} \right) \left(\frac{u^{0;N_i Z_i}_{q_i,\Lambda_i}}{\sqrt{n^{0;N_i Z_i}_{\Lambda_i}}} \right)$$

Matrix elements of the double beta transition operators between particle number and angular momentum projected states

Axial quadrupole deformation and mixing

$$\frac{\langle 0; N_f Z_f; q_f | \hat{O}^{0\nu\beta\beta}_{\xi} | 0; N_i Z_i; q_i \rangle}{\sqrt{\langle 0; N_f Z_f; q_f | 0; N_f Z_f; q_f \rangle \langle 0; N_i Z_i; q_i | 0; N_i Z_i; q_i \rangle}}$$

A=150

T.R.R., Martínez-Pinedo, PRL 105, 252503 (2010)

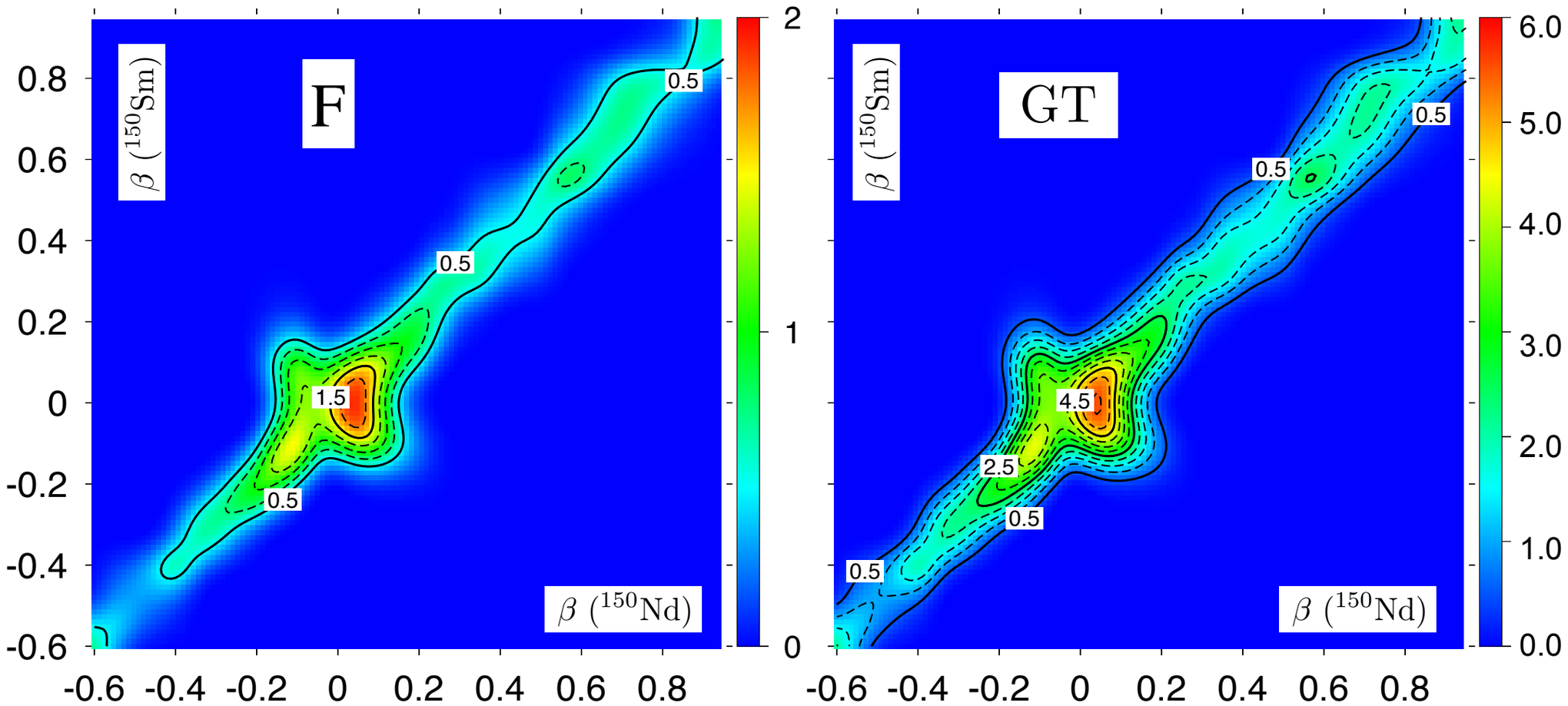

- GT strength greater than Fermi.
- Similar deformation between mother and granddaughter is favored by the transition operators
- Maxima are found close to sphericity although some other local maxima are found

Axial quadrupole deformation and mixing

$$\frac{\langle 0; N_f Z_f; q_f | \hat{O}^{0\nu\beta\beta}_{\xi} | 0; N_i Z_i; q_i \rangle}{\sqrt{\langle 0; N_f Z_f; q_f | 0; N_f Z_f; q_f \rangle \langle 0; N_i Z_i; q_i | 0; N_i Z_i; q_i \rangle}}$$

T.R.R., Martínez-Pinedo, PRL 105, 252503 (2010)

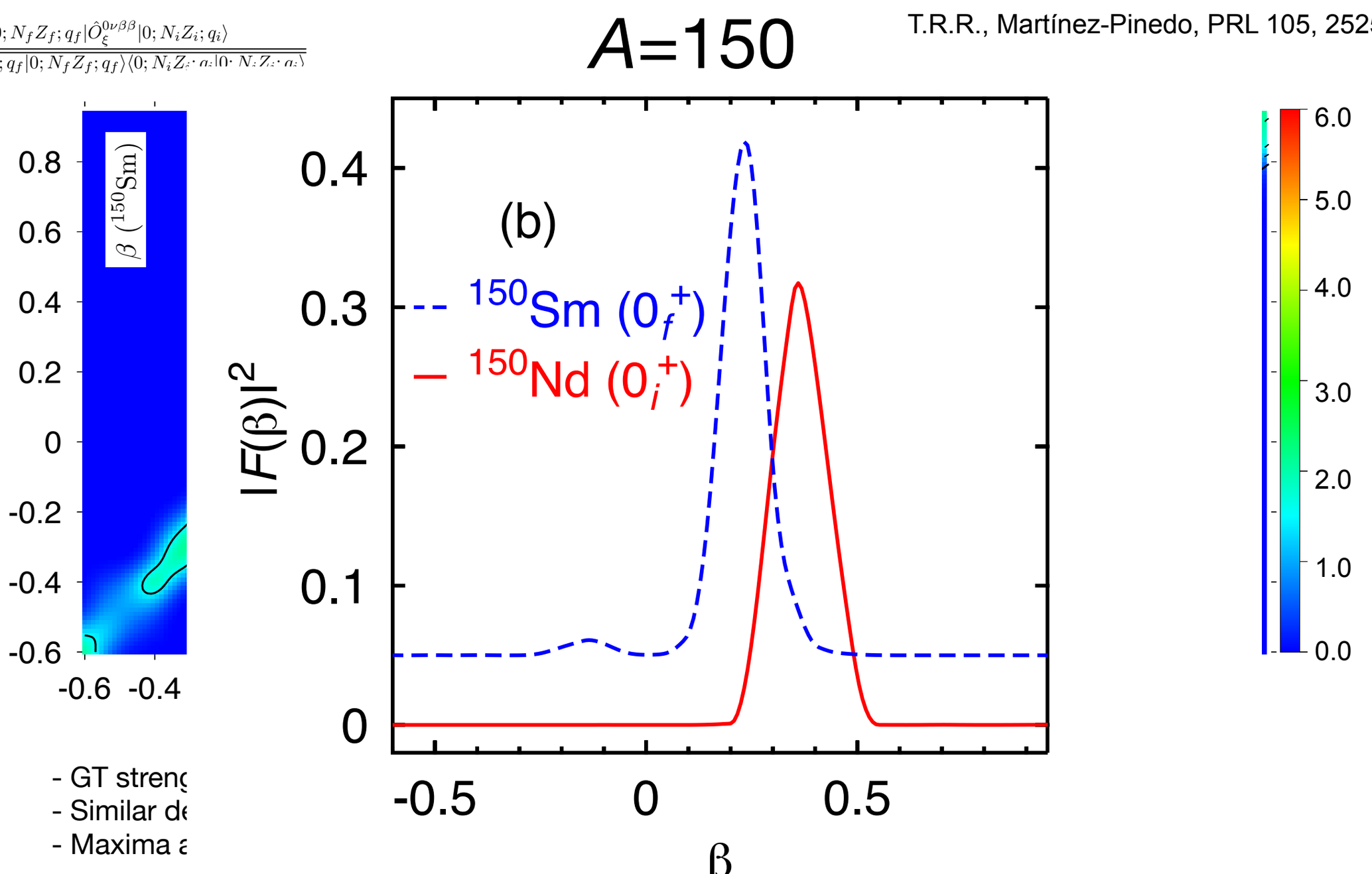

- GT streng
- Similar de
- Maxima a

- Final result depends on the distribution of probability of the corresponding initial and final collective states within this plot

Axial quadrupole deformation and mixing

$$\frac{\langle 0; N_f Z_f; q_f | \hat{O}^{0\nu\beta\beta}_{\xi} | 0; N_i Z_i; q_i \rangle}{\sqrt{\langle 0; N_f Z_f; q_f | 0; N_f Z_f; q_f \rangle \langle 0; N_i Z_i; q_i | 0; N_i Z_i; q_i \rangle}}$$

A=150

T.R.R., Martínez-Pinedo, PRL 105, 252503 (2010)

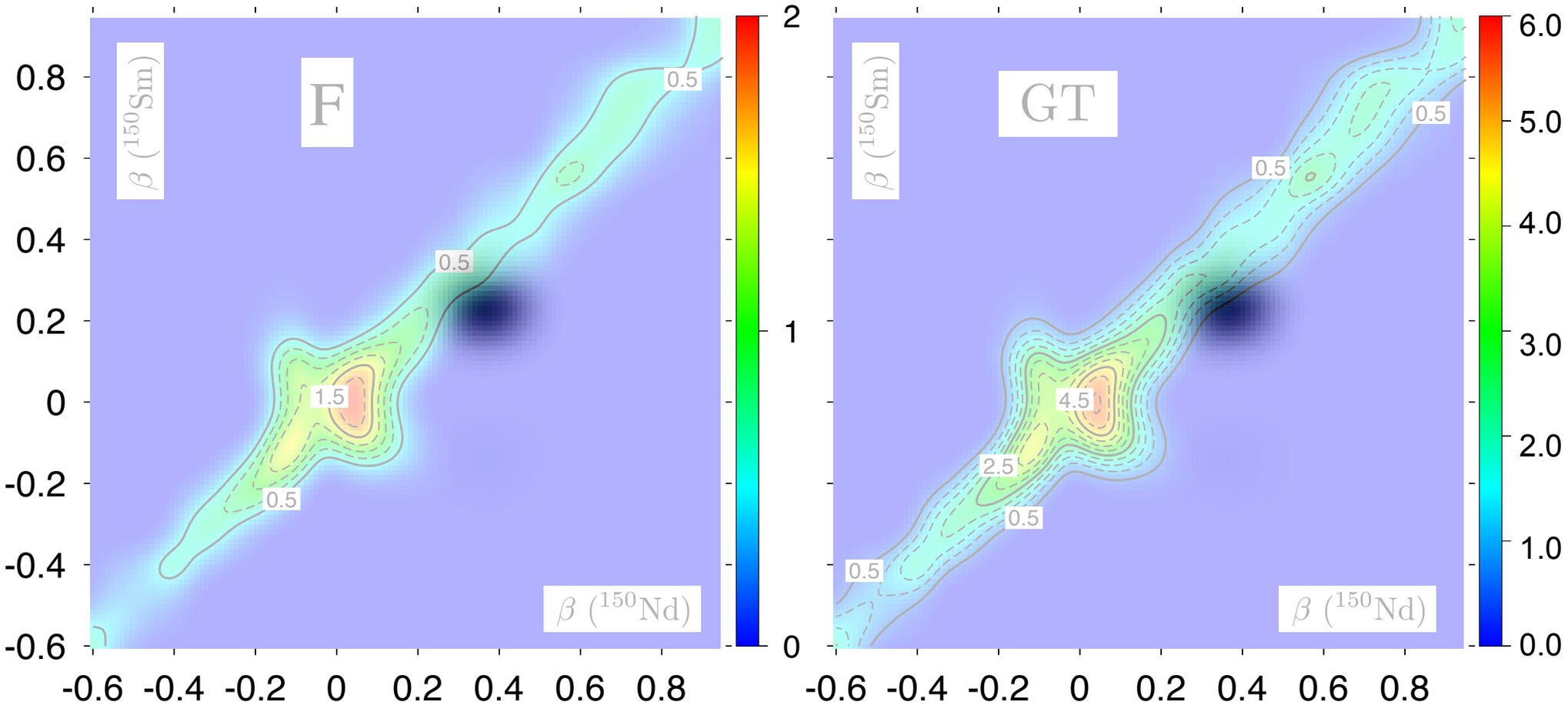

- GT strength greater than Fermi.
- Similar deformation between mother and granddaughter is favored by the transition operators
- Maxima are found close to sphericity although some other local maxima are found
- Final result depends on the distribution of probability of the corresponding initial and final collective states within this plot

Axial quadrupole deformation and mixing

$$\frac{\langle 0; N_f Z_f; q_f | \hat{O}^{0\nu\beta\beta}_{\xi} | 0; N_i Z_i; q_i \rangle}{\sqrt{\langle 0; N_f Z_f; q_f | 0; N_f Z_f; q_f \rangle \langle 0; N_i Z_i; q_i | 0; N_i Z_i; q_i \rangle}}$$

A=150

T.R.R., Martínez-Pinedo, PRL 105, 252503 (2010)

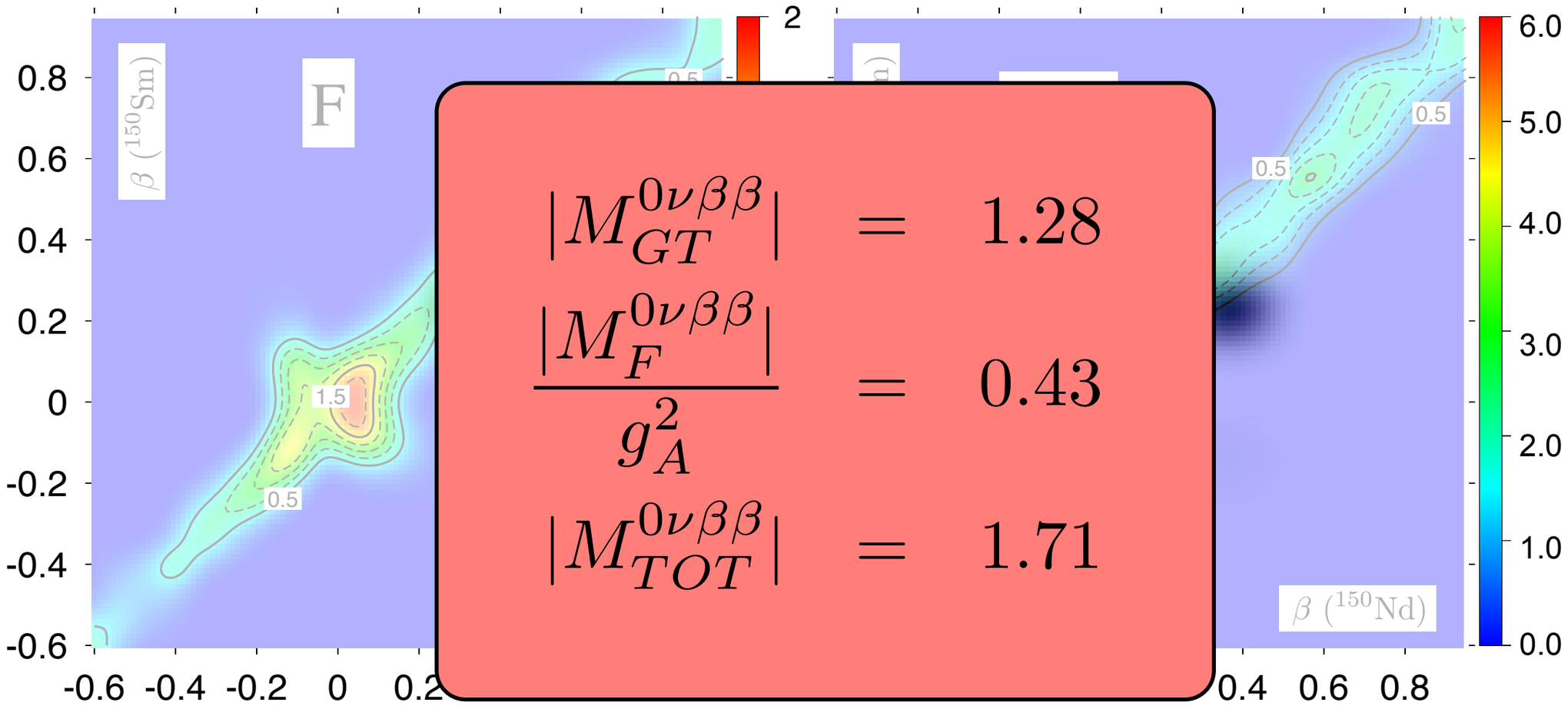

$$|M^{0\nu\beta\beta}_{GT}| = 1.28$$

$$\frac{|M^{0\nu\beta\beta}_{F}|}{g_A^2} = 0.43$$

$$|M^{0\nu\beta\beta}_{TOT}| = 1.71$$

- GT strength greater than Fermi.
- Similar deformation between mother and granddaughter is favored by the transition operators
- Maxima are found close to sphericity although some other local maxima are found
- Final result depends on the distribution of probability of the corresponding initial and final collective states within this plot

Axial quadrupole and octupole deformation and mixing

J. M. Yao and J. Engel, PRC 94, 014306 (2016)

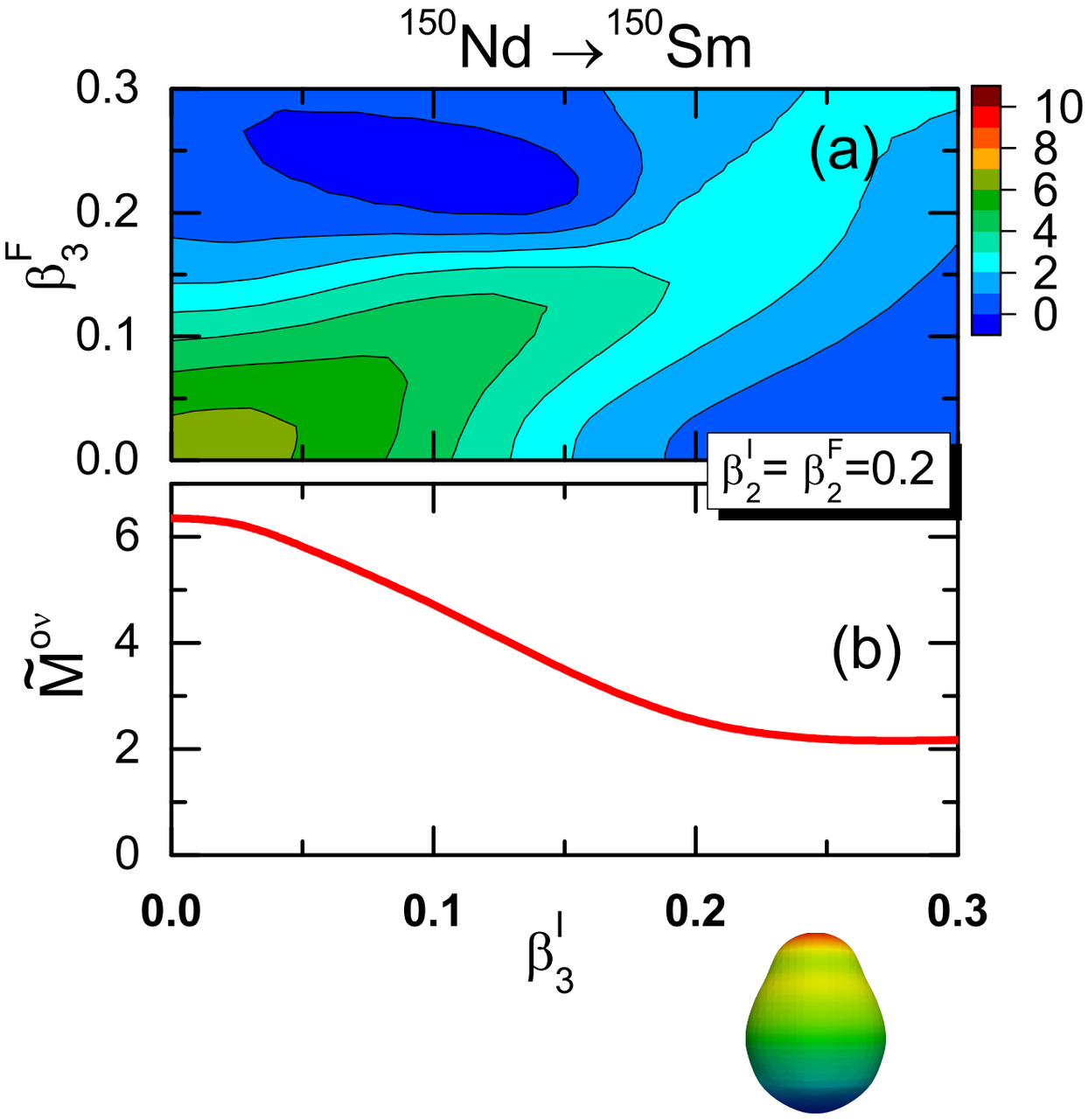

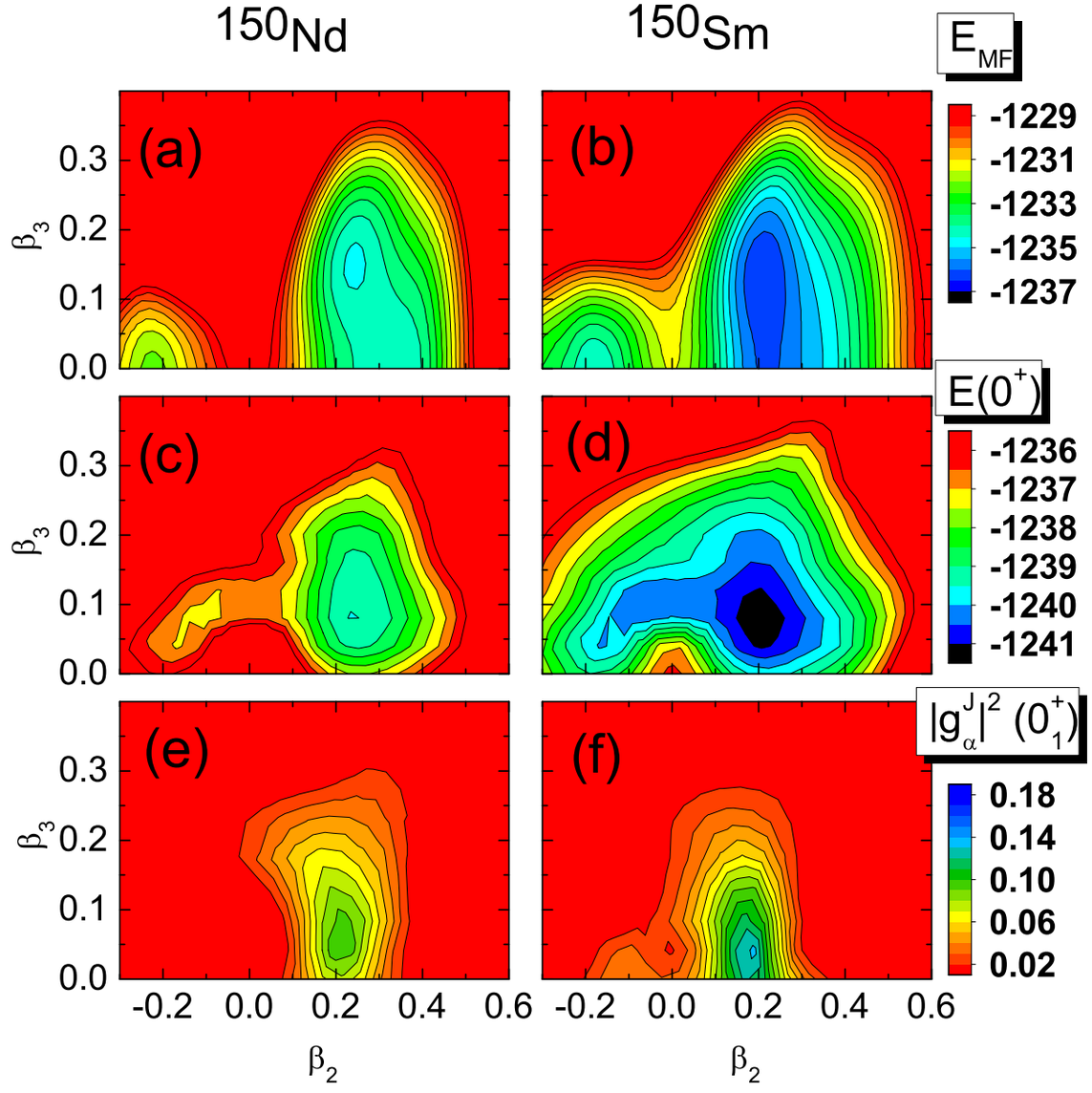

Axial quadrupole and octupole deformation and mixing

J. M. Yao and J. Engel, PRC 94, 014306 (2016)

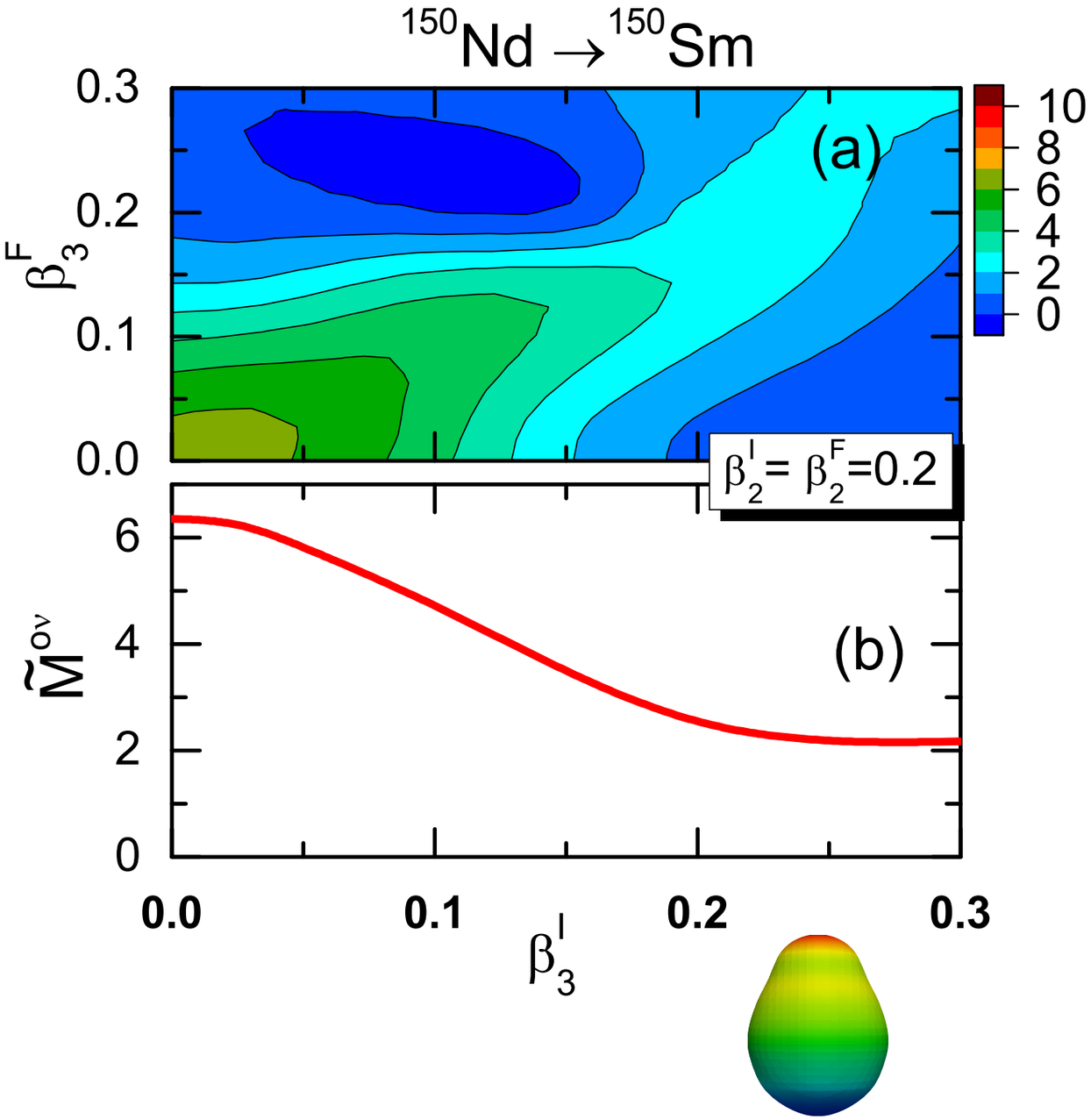

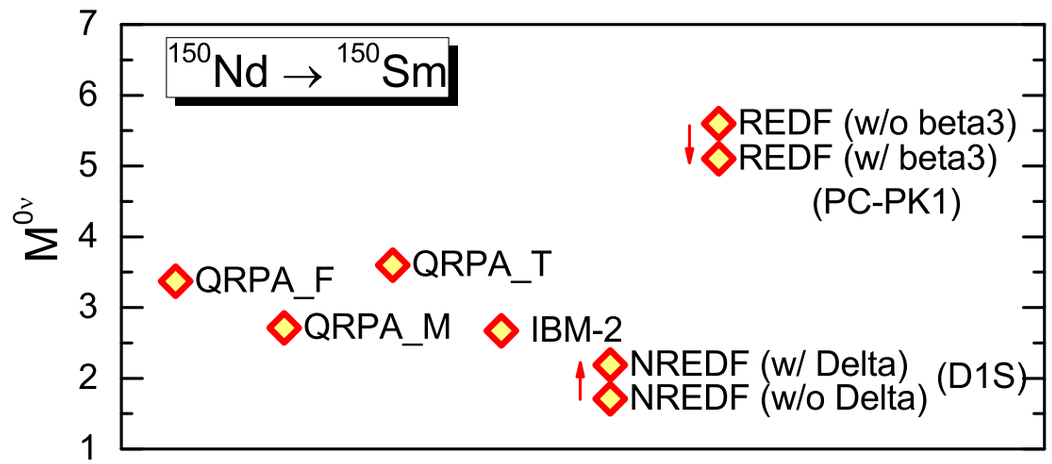

FIG. 5: (Color online) The final matrix element $M^{0\nu}$ from the GCM calculation with and without [46] octupole shape fluctuations (REDF) and those of the QRPA ("QRPA_F" [66], "QRPA_M" [45], "QRPA_T" [47]), the IMB-2 [67], and the non-relativistic GCM, based on the Gogny D1S interaction, with [68] and without [44] pairing fluctuations.

Axial+ triaxial quadrupole deformation and mixing

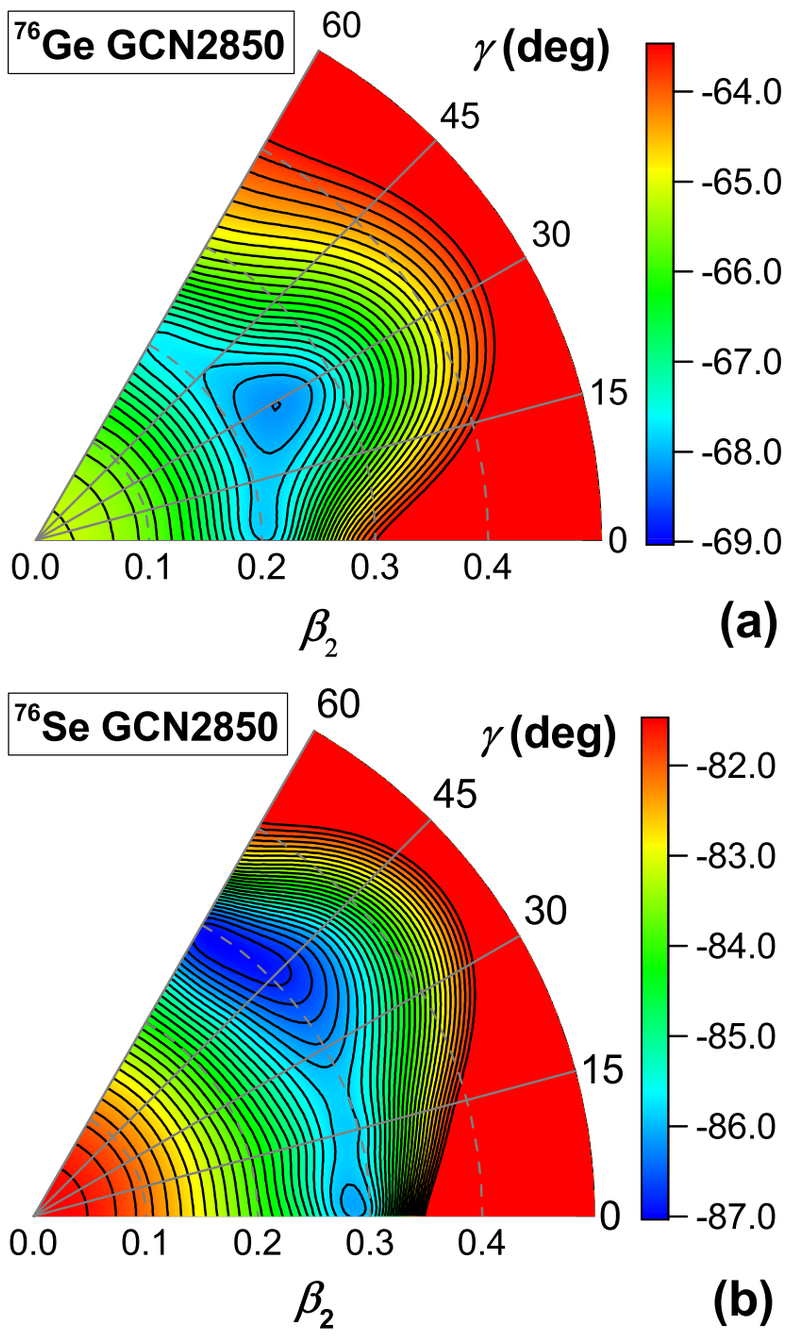

	GCN2850	JUN45
Axial GCM	2.93	3.51
Triaxial GCM	2.56	3.16

- Slight reduction of the NMEs in 76Ge decay.
- It could depend on the interaction.
- It will depend on the decaying isotope

⇒ a more systematic study is still needed.

C. F. Jiao, J. Engel, J. D. Holt, PRC 96, 054310 (2017)

Axial quadrupole deformation and pp/nn pairing fluctuations and mixing

Dependence on deformation

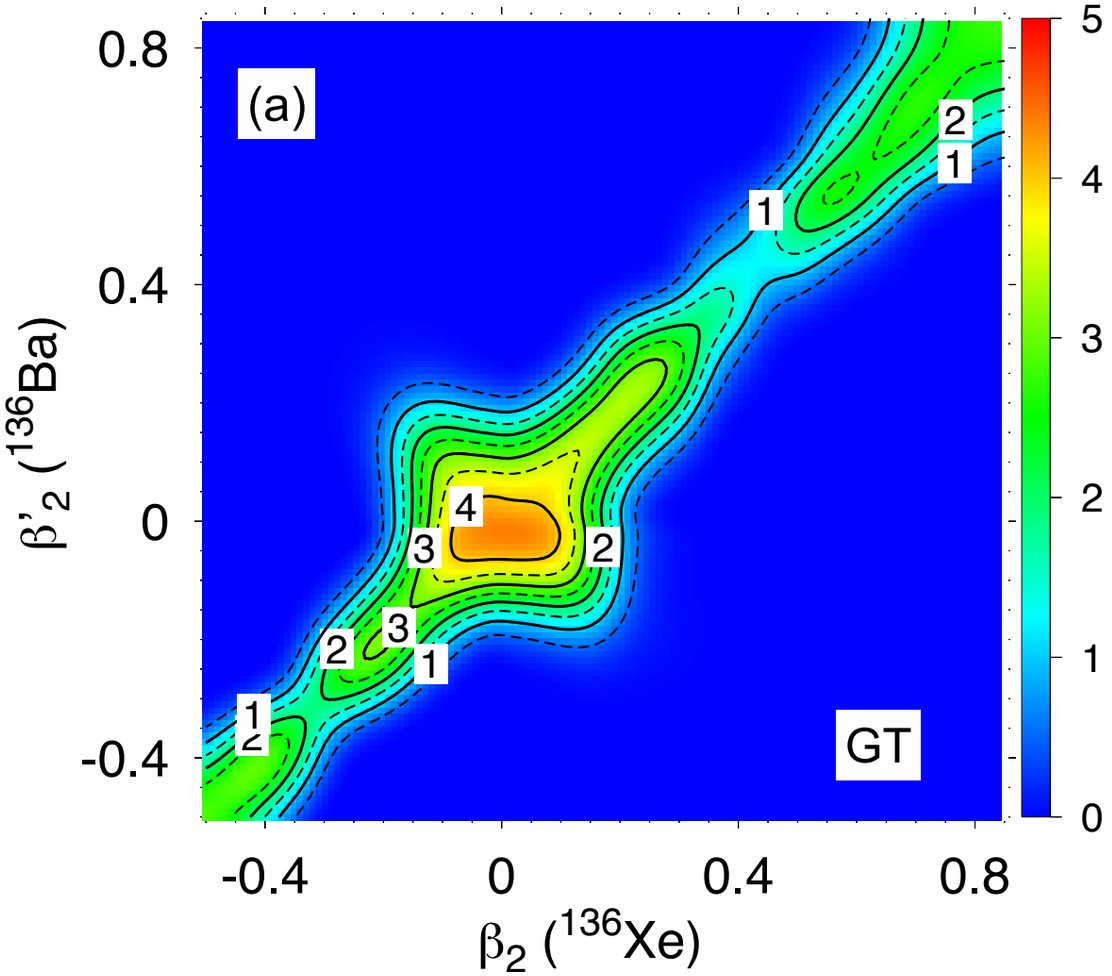

Dependence on pp/nn pairing

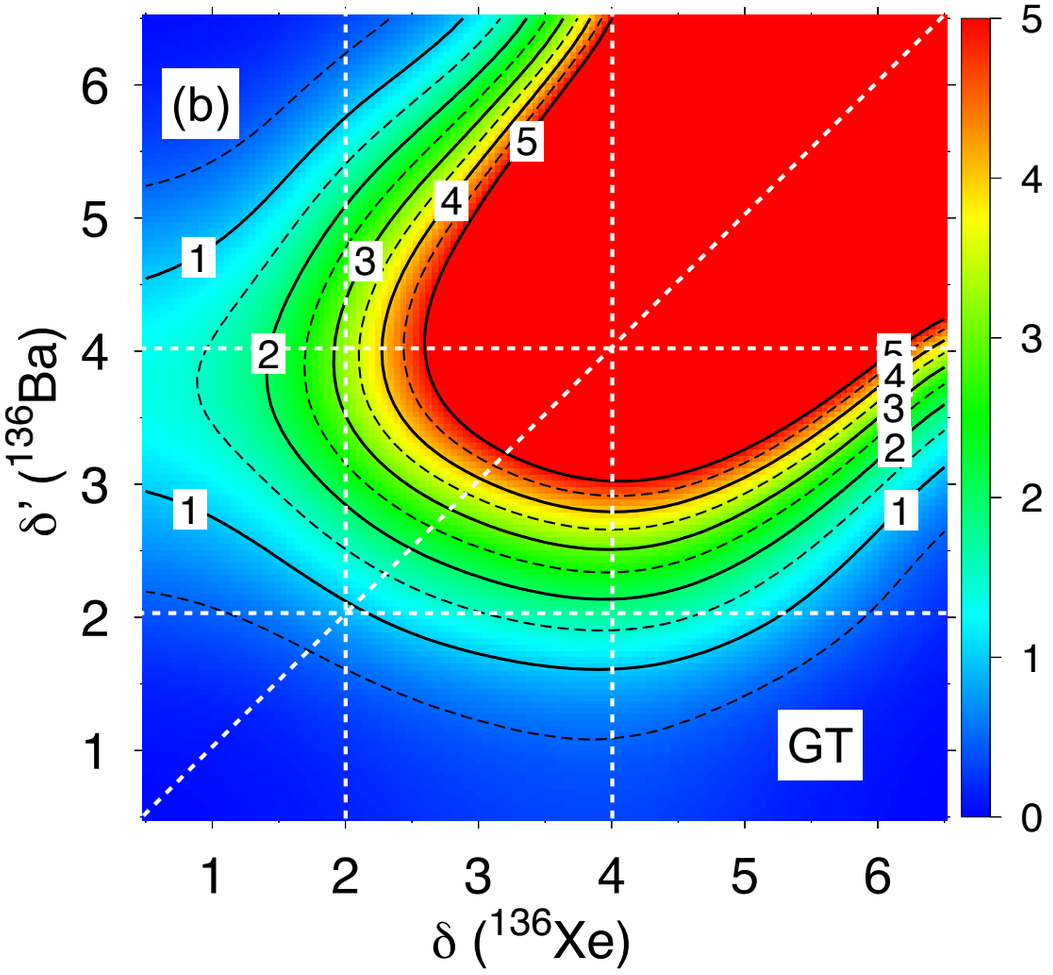

N. López-Vaquero, T.R.R., J.L. Egido, PRL 111, 142501 (2013)

Axial quadrupole deformation and pp/nn pairing fluctuations and mixing

Isotope	$\Delta Q(\beta_2)$	$\Delta Q(\beta_2,\delta)$	$M^{0\nu}(\beta_2)$	$M^{0\nu}(\beta_2,\delta)$	Var (%)	$\frac{T_{1/2}(\beta_2,\delta)}{T_{1/2}(\beta_2)}$
^{48}Ca	0.265	0.131	$2.370^{1.914}_{0.456}$	$2.229^{1.797}_{0.431}$	-6	1.13
^{76}Ge	0.271	0.190	$4.601^{3.715}_{0.886}$	$5.551^{4.470}_{1.082}$	21	0.69
^{82}Se	-0.366	-0.246	$4.218^{3.381}_{0.837}$	$4.674^{3.743}_{0.931}$	11	0.81
^{96}Zr	2.580	2.628	$5.650^{4.618}_{1.032}$	$6.498^{5.296}_{1.202}$	15	0.76
^{100}Mo	1.879	1.757	$5.084^{4.149}_{0.935}$	$6.588^{5.361}_{1.227}$	30	0.60
^{116}Cd	1.365	1.337	$4.795^{3.931}_{0.864}$	$5.348^{4.372}_{0.976}$	12	0.80
^{124}Sn	-0.830	-0.687	$4.808^{3.893}_{0.916}$	$5.787^{4.680}_{1.107}$	20	0.69
^{128}Te	-0.564	-0.594	$4.107^{3.079}_{1.027}$	$5.687^{4.255}_{1.432}$	38	0.52
^{130}Te	-0.348	-0.628	$5.130^{4.141}_{0.989}$	$6.405^{5.161}_{1.244}$	25	0.64
^{136}Xe	-1.027	-0.787	$4.199^{3.673}_{0.526}$	$4.773^{4.170}_{0.604}$	14	0.77
^{150}Nd	-0.380	-0.282	$1.707^{1.278}_{0.429}$	$2.190^{1.639}_{0.551}$	29	0.61

N. López-Vaquero, T.R.R., J.L. Egido, PRL 111, 142501 (2013)

Axial quadrupole deformation and pn pairing fluctuations and mixing

$$H = h_0 - \sum_{\mu=-1}^{1} g_\mu^{T=1}\, S_\mu^\dagger S_\mu - \frac{\chi}{2}\sum_{K=-2}^{2} Q_{2K}^\dagger Q_{2K}$$
$$- g^{T=0}\sum_{\nu=-1}^{1} P_\nu^\dagger P_\nu + g_{ph}\sum_{\mu,\nu=-1}^{1} F_\nu^{\mu\dagger} F_\nu^\mu\,, \qquad (2)$$

where h_0 contains spherical single particle energies, Q_{2K} are the components of a quadrupole operator defined in Ref. [15], and

$$S_\mu^\dagger = \frac{1}{\sqrt{2}}\sum_l \hat{l}[c_l^\dagger c_l^\dagger]_{00\mu}^{001}\,, \quad P_\mu^\dagger = \frac{1}{\sqrt{2}}\sum_l \hat{l}[c_l^\dagger c_l^\dagger]_{0\mu0}^{010}\,,$$
$$F_\nu^\mu = \frac{1}{2}\sum_i \sigma_i^\mu \tau_i^\nu = \sum_l \hat{l}[c_l^\dagger \bar{c}_l]_{0\mu\nu}^{011}\,. \qquad (3)$$

$$H' = H - \lambda_Z N_Z - \lambda_N N_N - \lambda_Q Q_{20} - \frac{\lambda_P}{2}\left(P_0 + P_0^\dagger\right)\,, \quad (6)$$

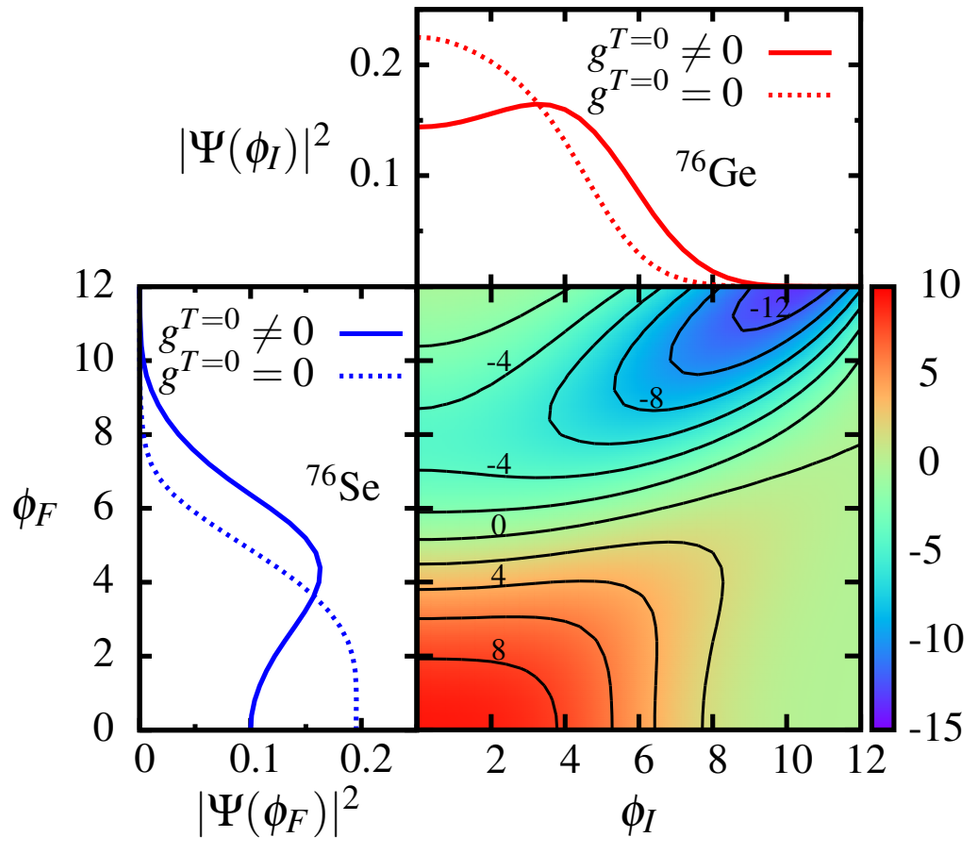

FIG. 3. (Color online.) **Bottom right:** $\mathcal{N}_{\phi_I}\mathcal{N}_{\phi_F}\langle\phi_F|\mathcal{P}_F\hat{M}_{0\nu}\mathcal{P}_I|\phi_I\rangle$ for projected quasiparticle vacua with different values of the initial and final isoscalar pairing amplitudes ϕ_I and ϕ_F, from the SkO′-based interaction (see text). **Top and bottom left:** Square of collective wave functions in ^{76}Ge and ^{76}Se.

N. Hinohara and J. Engel, PRC 031031(R) (2014)

Axial quadrupole deformation and pn pairing fluctuations and mixing

$$H = h_0 - \sum_{\mu=-1}^{1} g_\mu^{T=1}\, S_\mu^\dagger S_\mu - \frac{\chi}{2} \sum_{K=-2}^{2} Q_{2K}^\dagger Q_{2K}$$

$$- g^{T=0} \sum_{\nu=-1}^{1} P_\nu^\dagger P_\nu +$$

where h_0 contains spherical
are the components of a qu
Ref. [15], and

$$S_\mu^\dagger = \frac{1}{\sqrt{2}} \sum_l \hat{l} [c_l^\dagger c_l^\dagger]_{00\mu}^{001} ,$$

$$F_\nu^\mu = \frac{1}{2} \sum_i \sigma_i^\mu \tau_i^\nu = \sum_l \hat{l} [c_l^\dagger \bar{c}_l]_{0\mu\nu}^{011} . \qquad (3)$$

$$H' = H - \lambda_Z N_Z - \lambda_N N_N - \lambda_Q Q_{20} - \frac{\lambda_P}{2} \left(P_0 + P_0^\dagger \right) , \quad (6)$$

Exploring explicitly pp/nn and pn pairing could produce cancellations

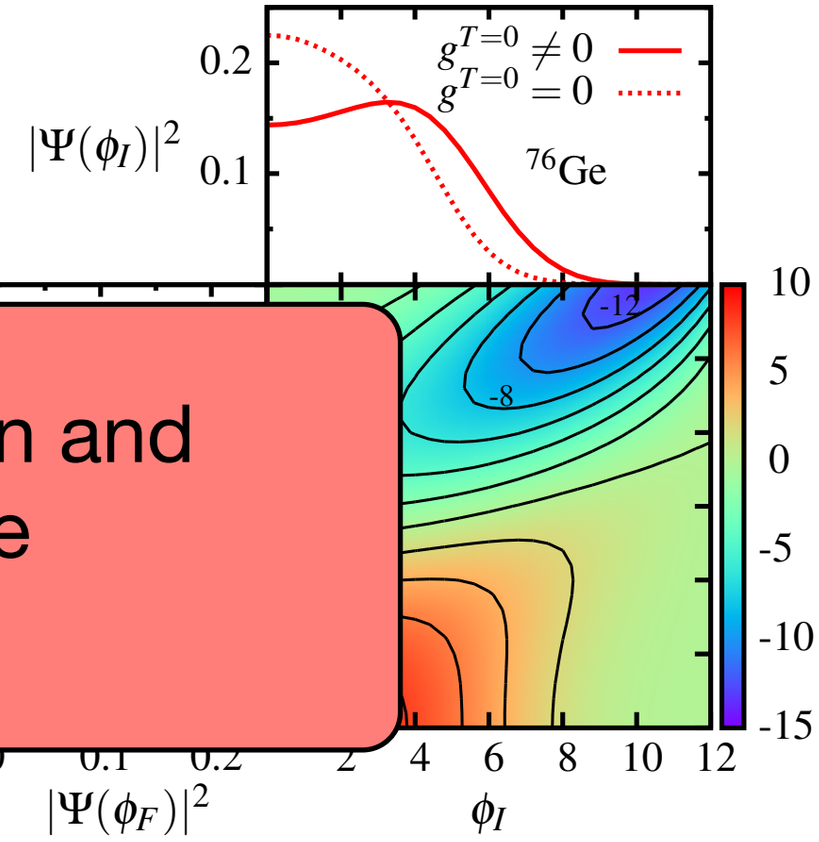

FIG. 3. (Color online.) **Bottom right:** $\mathcal{N}_{\phi_I}\mathcal{N}_{\phi_F} \langle \phi_F | \mathcal{P}_F \hat{M}_{0\nu} \mathcal{P}_I | \phi_I \rangle$ for projected quasiparticle vacua with different values of the initial and final isoscalar pairing amplitudes ϕ_I and ϕ_F, from the SkO′-based interaction (see text). **Top and bottom left:** Square of collective wave functions in ^{76}Ge and ^{76}Se.

N. Hinohara and J. Engel, PRC 031031(R) (2014)

Proton-neutron pairing in the Interacting Shell Model

J. Menéndez, et al., PRC 93, 014305 (2016).

$$H_{\rm coll} = H_M + g^{T=1} \sum_{n=-1}^{1} S_n^\dagger S_n + g^{T=0} \sum_{m=-1}^{1} P_m^\dagger P_m$$

$$+ g_{ph} \sum_{m,n=-1}^{1} :\mathcal{F}_{mn}^\dagger \mathcal{F}_{mn}: + \chi \sum_{\mu=-2}^{2} :Q_\mu^\dagger Q_\mu:$$

- Increase of the NME when isoscalar pairing is removed.
- Further increase when spin-isospin is also removed

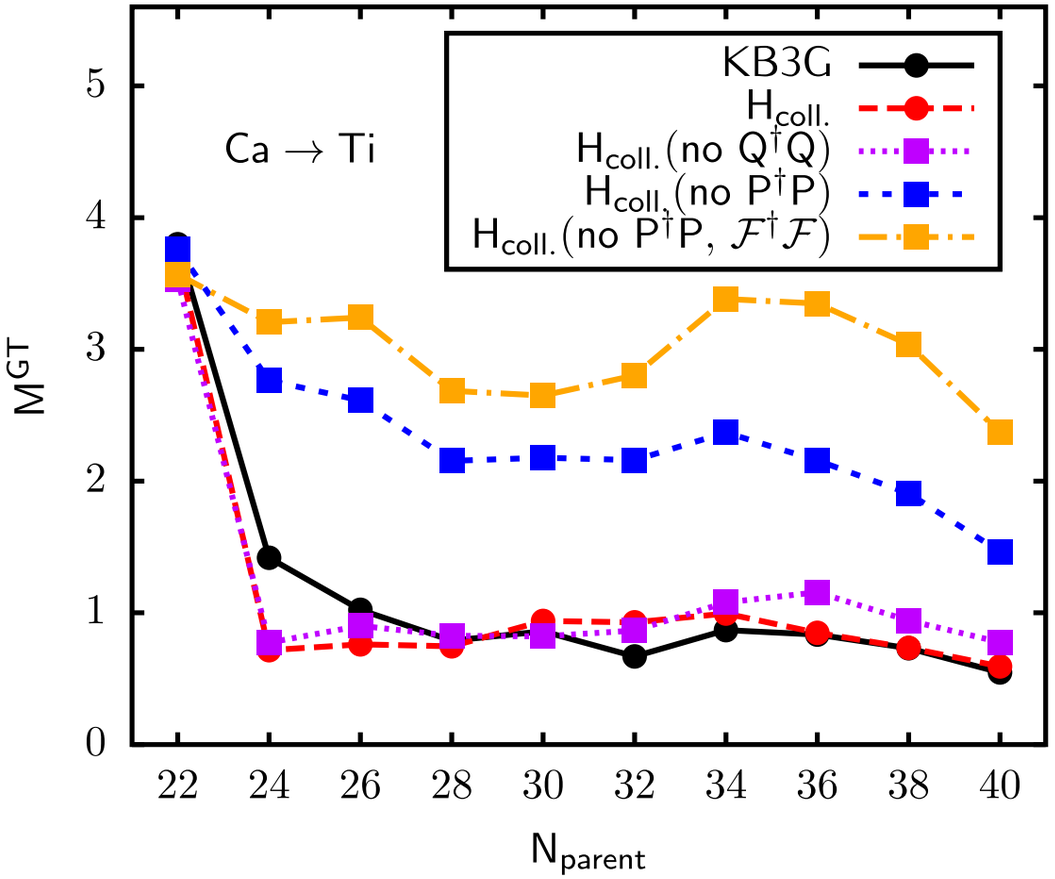

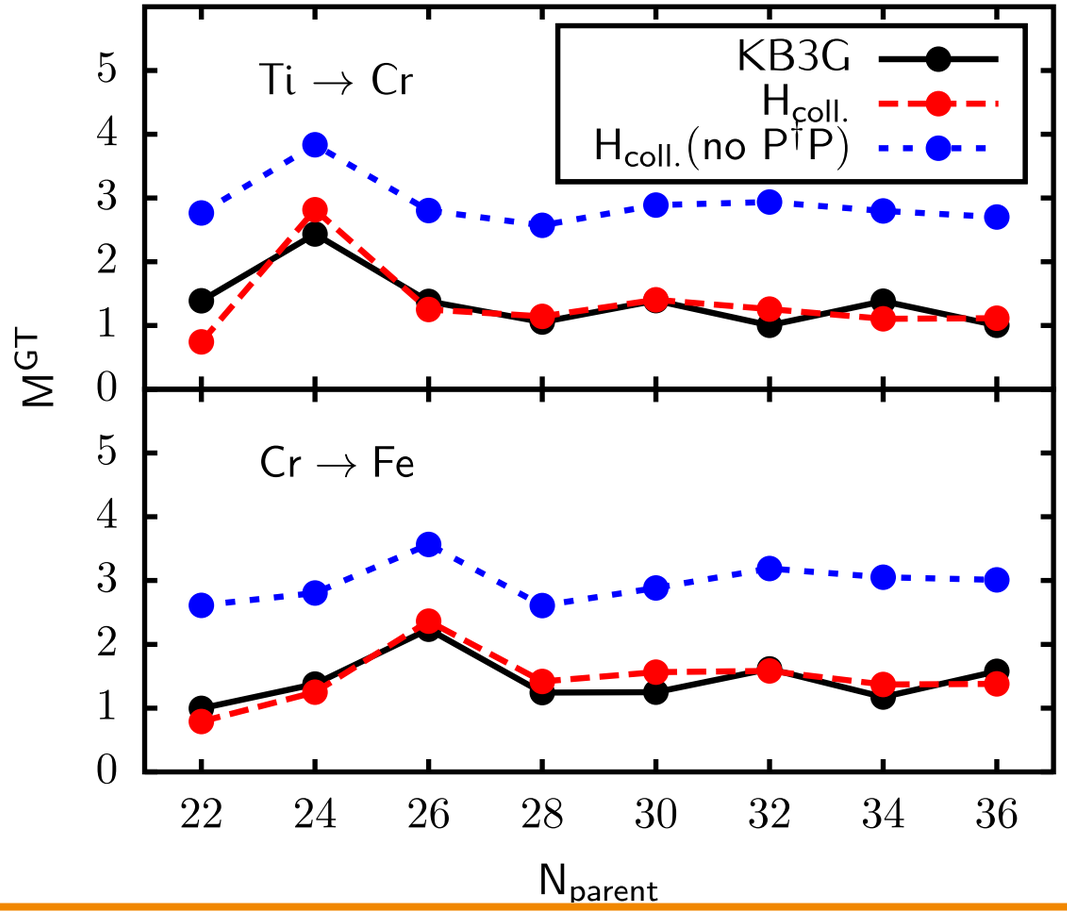

Valence space

Shell Model (SM) calculations

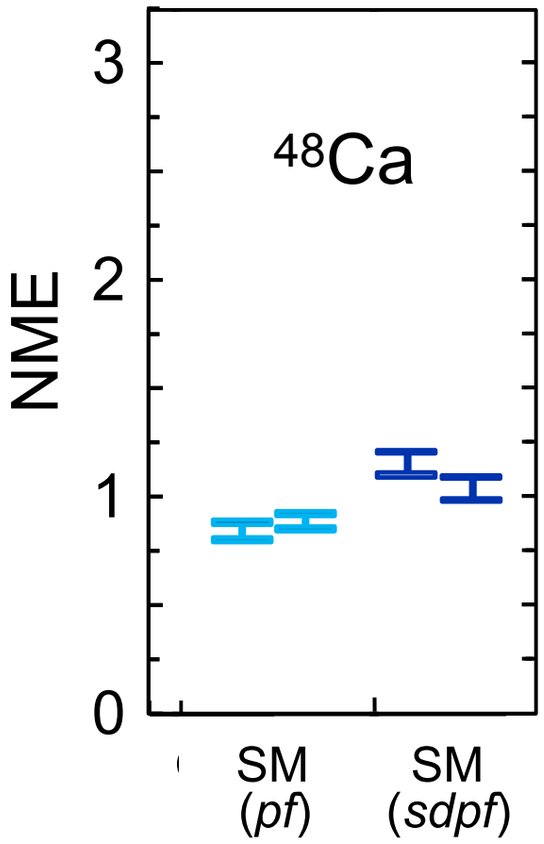

Y. Iwata et al., PRL 116, 112502 (2016)

Shell Model and GCM calculations

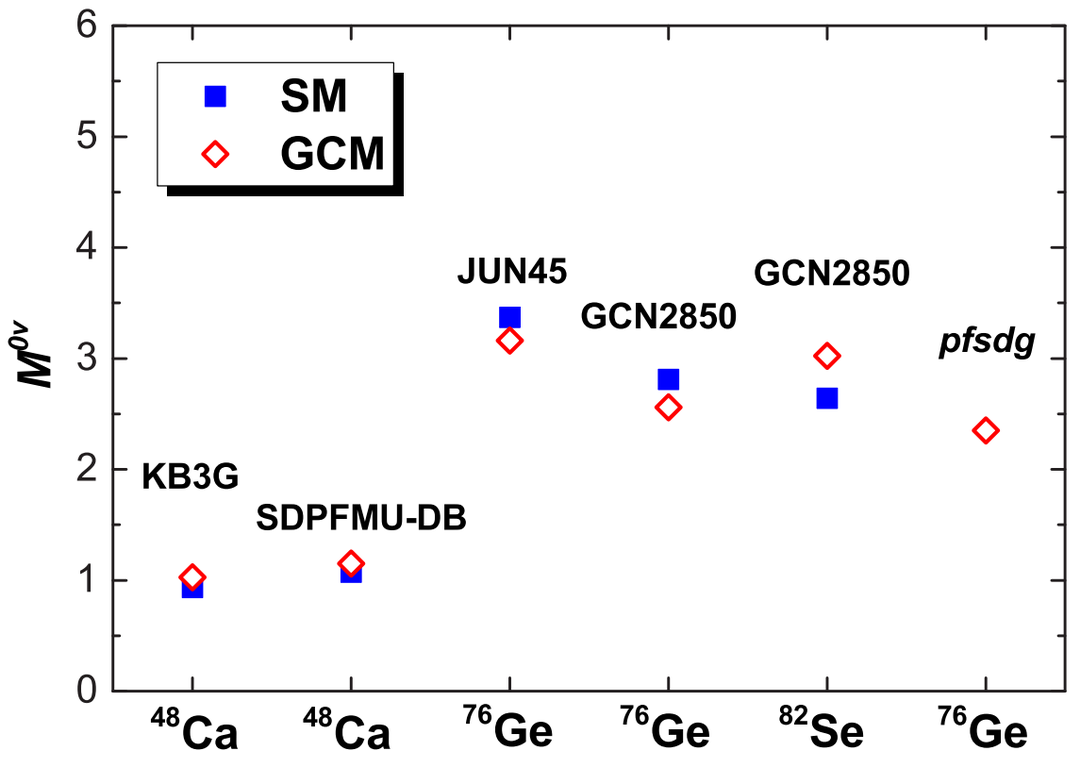

C. F. Jiao, J. Engel, J. D. Holt, PRC 96, 054310 (2017)

- Small influence by increasing the valence space.
- Larger (than two-shell) valence spaces and more systematic calculations are still needed.

Differences between GCM and Interacting Shell Model

Where do the differences between GCM and Interacting Shell Model come from?

NMEs without correlations

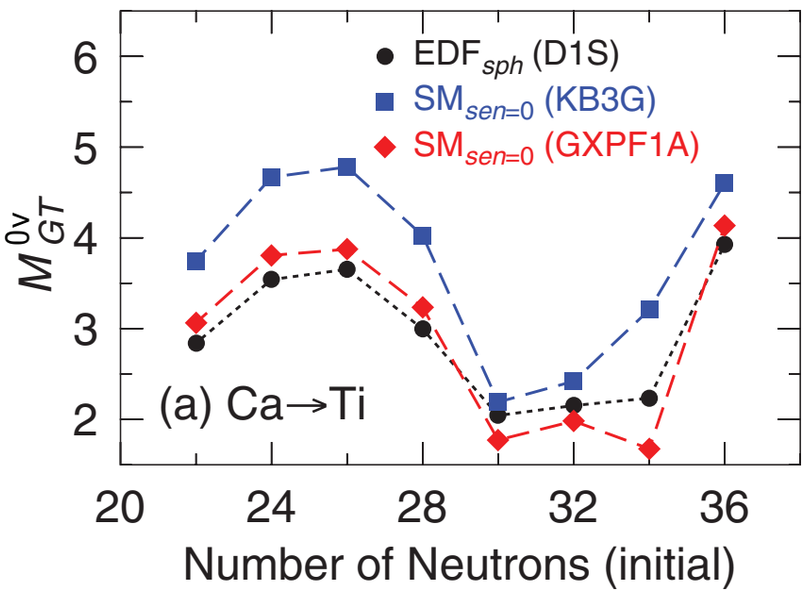

- Same pattern in spherical EDF, seniority 0 Shell Model, and Generalized Seniority model (overall scale?)

NMEs with correlations

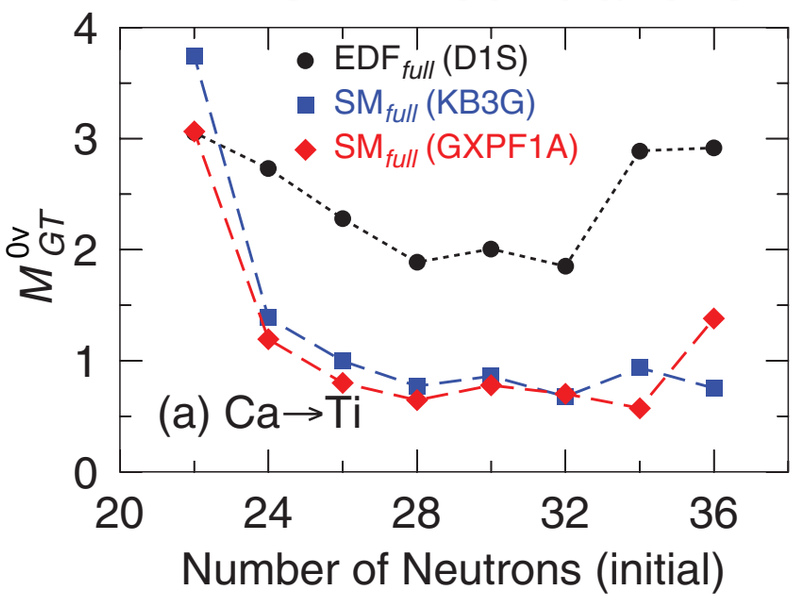

- GCM results are systematically larger

J. Menéndez, T. R. R., A. Poves, G. Martínez-Pinedo, PRC 90, 024311 (2014).

Differences between GCM and Interacting Shell Model

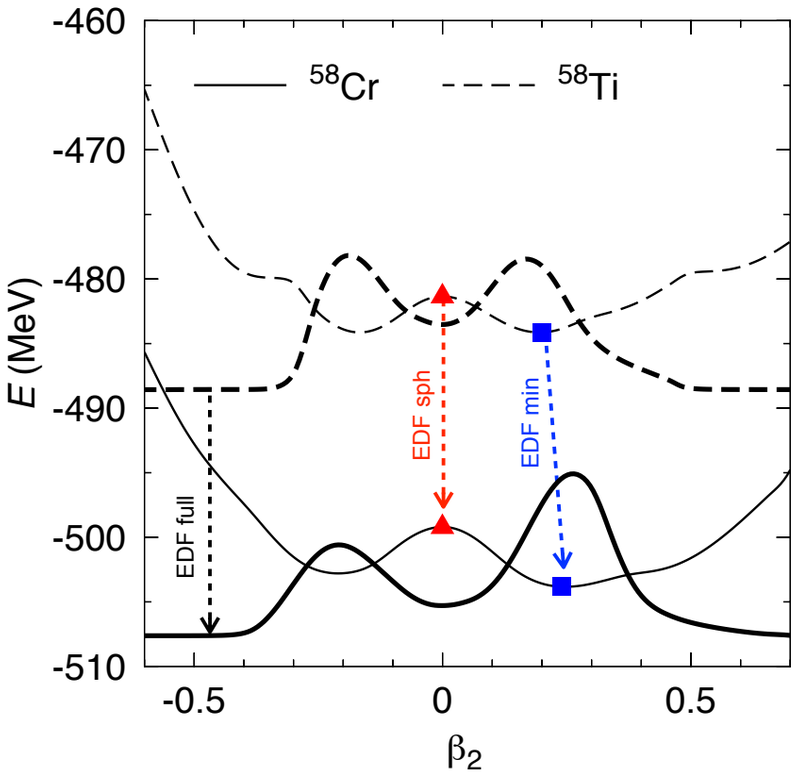

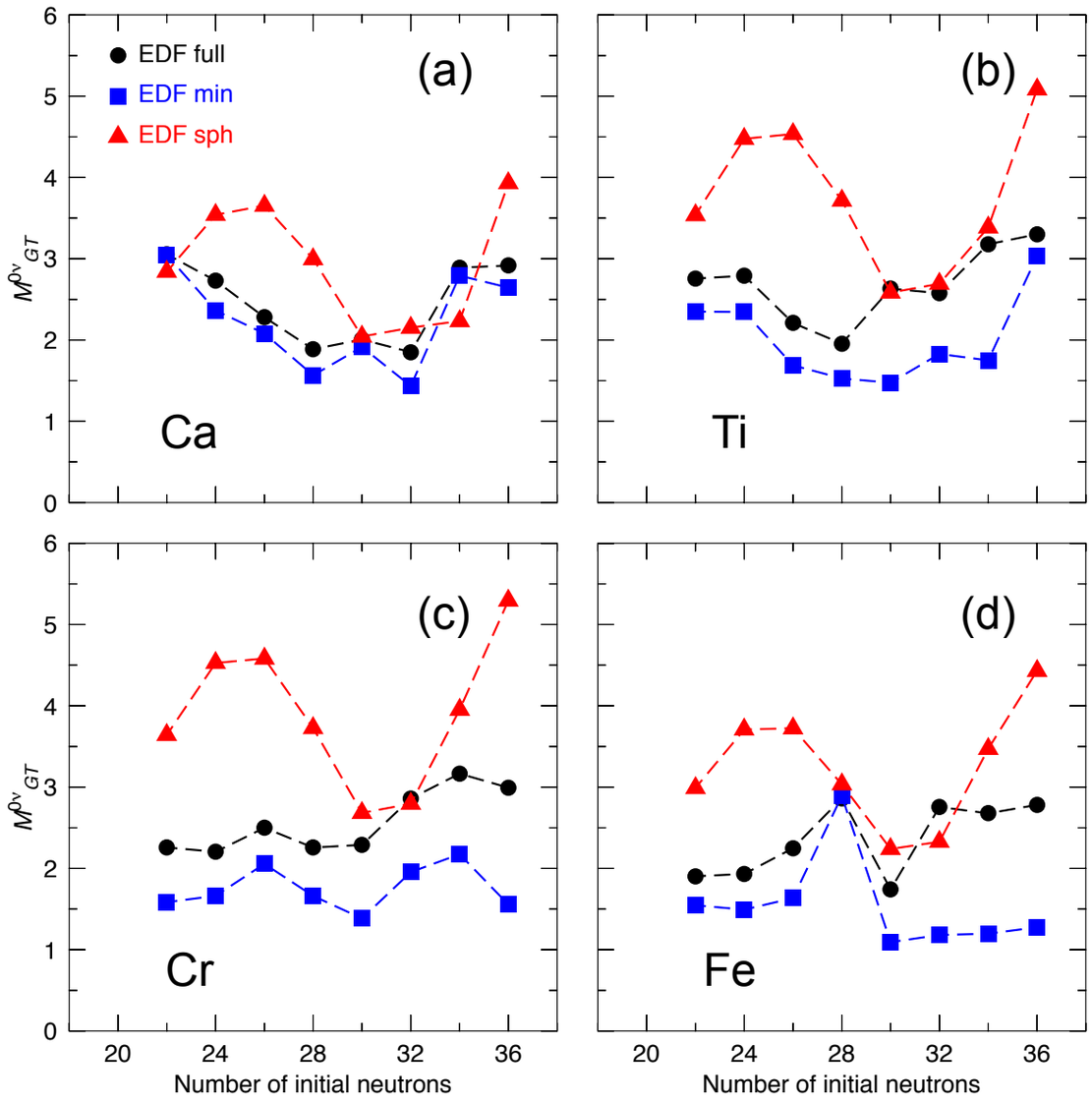

J. Menéndez, T. R. R., A. Poves, G. Martínez-Pinedo, PRC 90, 024311 (2014).

Differences between GCM and Interacting Shell Model

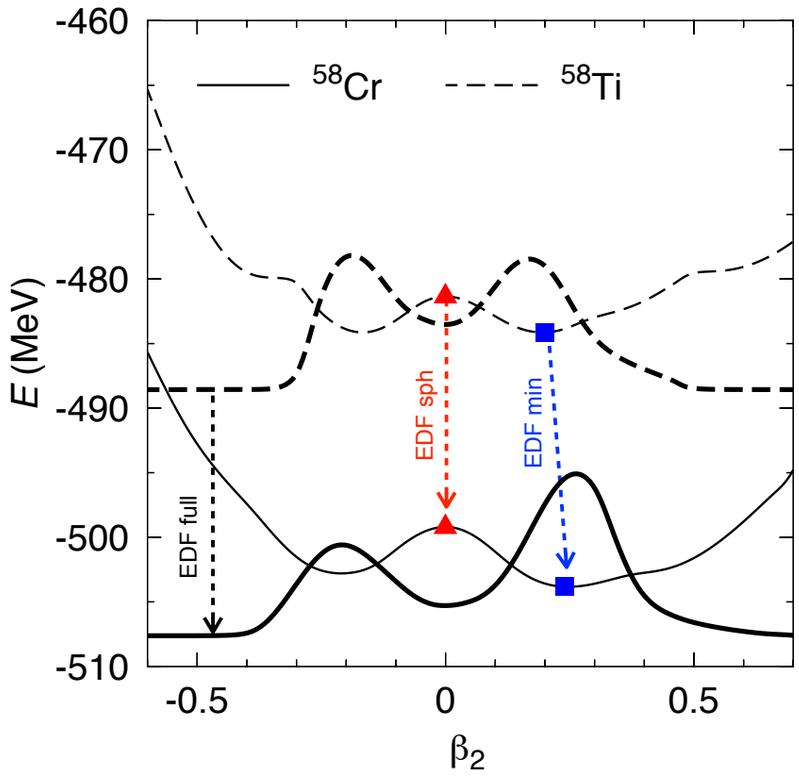

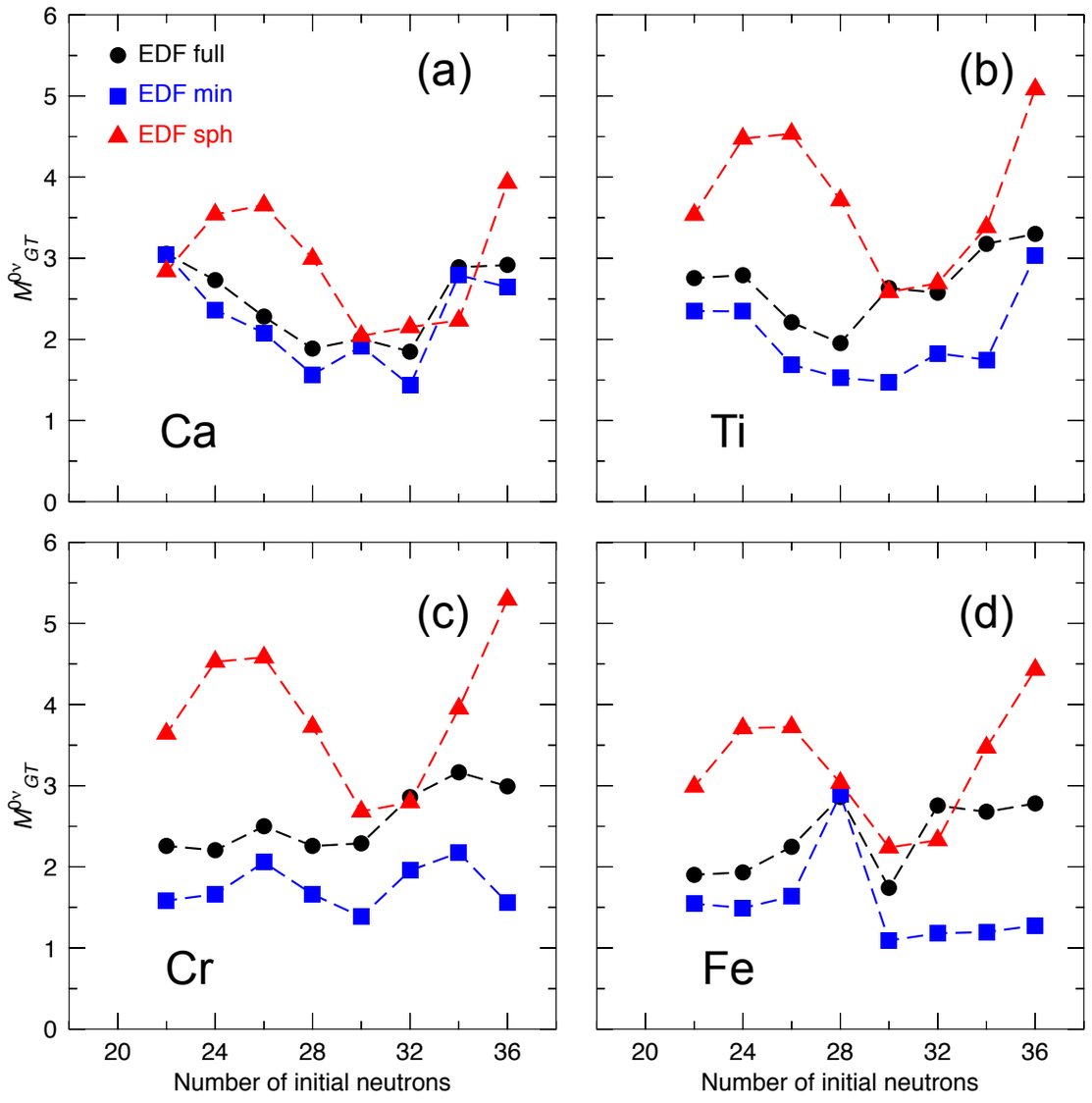

- NMEs are reduced with respect to the spherical value when correlations are included.

- The biggest reduction is produced by angular momentum restoration and configuration mixing produces an increase of the NME.

J. Menéndez, T. R. R., A. Poves, G. Martínez-Pinedo, PRC 90, 024311 (2014).

Differences between GCM and Interacting Shell Model

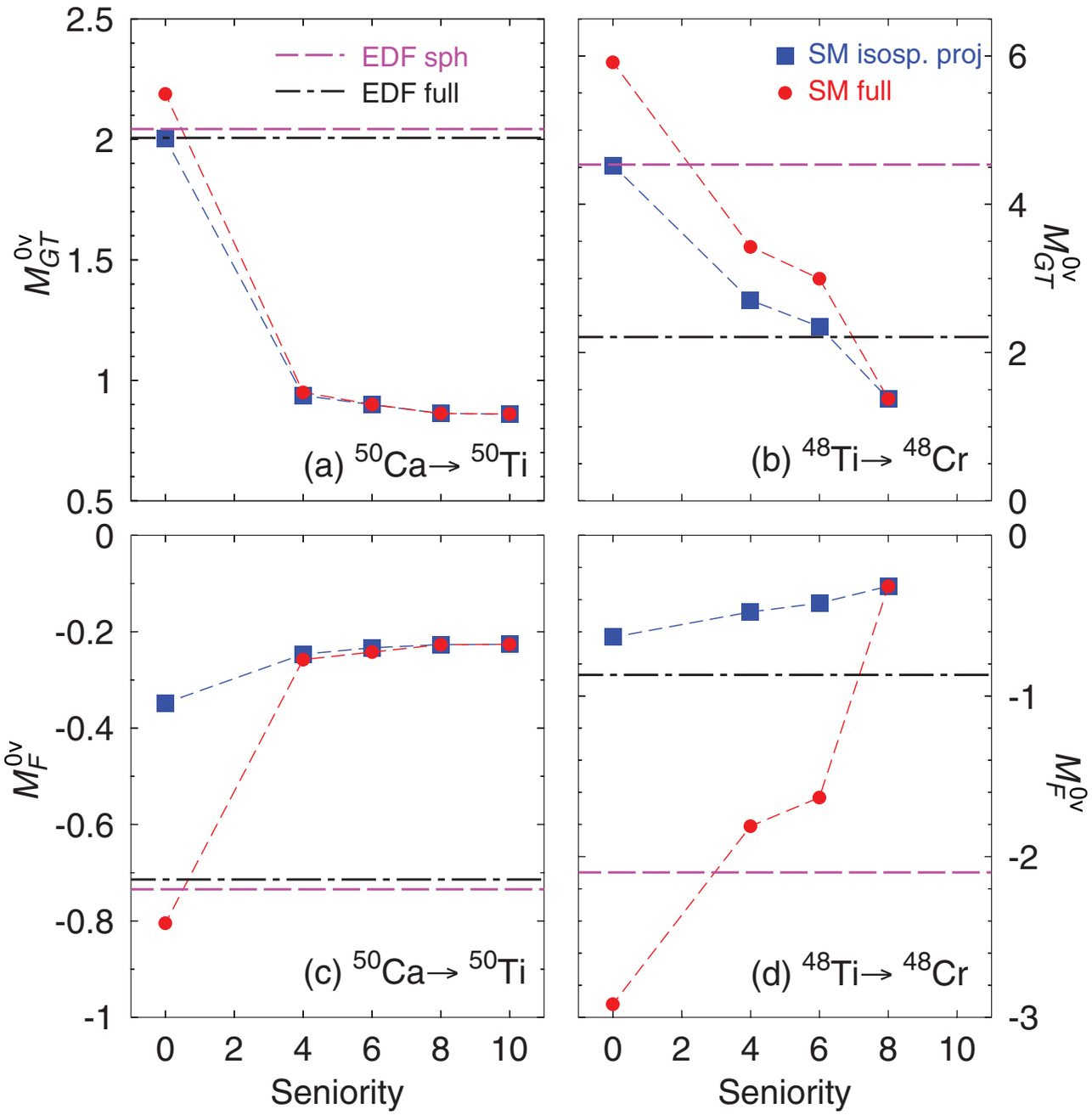

J. Menéndez, T. R. R., A. Poves, G. Martínez-Pinedo, PRC 90, 024311 (2014).

Differences between GCM and Interacting Shell Model

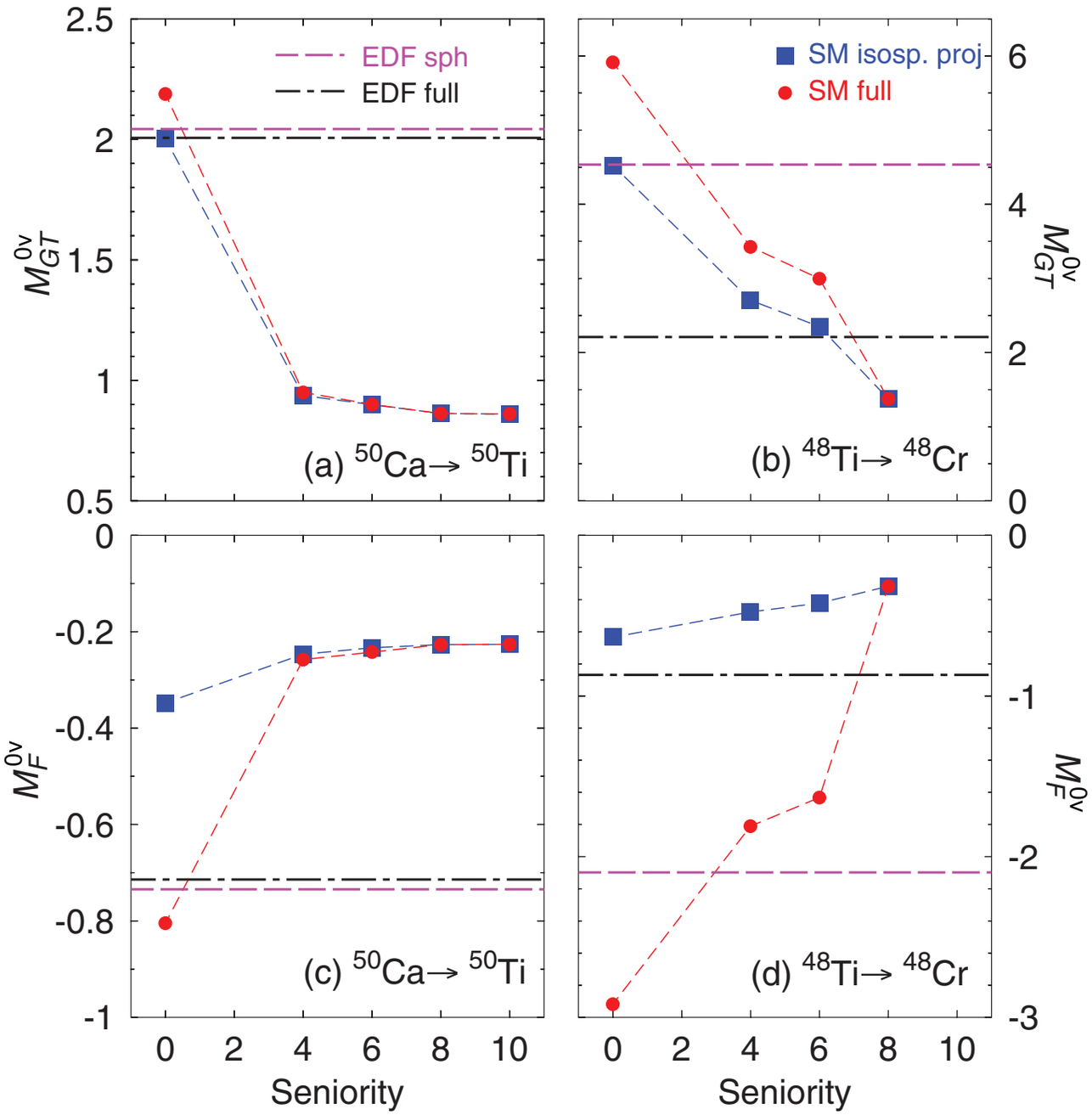

- The biggest reduction (in Shell model calculations) is produced by including higher seniority components in the nuclear wave functions.
- Isospin projection is relevant for the Fermi part of the NME and less important for the Gamow-Teller part.
- Isospin projection tends to reduce the NME.
- EDF does not include properly those higher seniority components, specially in spherical nuclei.

J. Menéndez, T. R. R., A. Poves, G. Martínez-Pinedo, PRC 90, 024311 (2014).

Summary

- **NMEs differ a factor of three between the different methods but we need to understand which are the pros/cons of each method to provide reliable numbers (precision vs. accuracy).**

- **Nuclear physics aspects like deformation, pairing, shell effects, etc., are understood similarly within different approaches.**

- **Systematic comparisons between ISM/GCM methods have been performed and they tend to agree when appropriate deformation and pairing correlations are taken into account in GCM approaches.**

- **Other effects like using consistent operators and/or two-body currents ("g_a quenching") are important (A. Nicholson's talk)**

- **We hope that more constrained and reliable NMEs will be provided in the near future.**

Transition operator

- Relativistic form

$$\mathcal{H}_{\rm weak}(x) = \frac{G_F \cos\theta_C}{\sqrt{2}} j^\mu(x)\mathcal{J}^\dagger_\mu(x) + \text{h.c.},$$

$$j^\mu(x) = \bar{e}(x)\gamma^\mu(1-\gamma_5)\nu_e(x).$$

$$\begin{aligned}\mathcal{J}^\dagger_\mu(x) &= \bar{\psi}(x)\Big[g_V(q^2)\gamma_\mu + \mathrm{i}g_M(q^2)\frac{\sigma_{\mu\nu}}{2m_p}q^\nu \\ &- g_A(q^2)\gamma_\mu\gamma_5 - g_P(q^2)q_\mu\gamma_5\Big]\tau_-\psi(x),\end{aligned}$$

$$M^{0\nu}(0^+_I \to 0^+_F) \equiv \langle 0^+_F|\hat{\mathcal{O}}^{0\nu}|0^+_I\rangle,$$

$$\hat{\mathcal{O}}^{0\nu} = \sum_i \hat{\mathcal{O}}^{0\nu}_i, \quad (i = VV, AA, AP, PP, MM)$$

$$\hat{\mathcal{O}}^{0\nu}_i = \frac{4\pi R}{g_A^2}\int d^3x_1 d^3x_2 \int \frac{d^3q}{(2\pi)^3}\frac{\mathrm{e}^{\mathrm{i}\boldsymbol{q}\cdot(\boldsymbol{x}_1-\boldsymbol{x}_2)}}{q(q+E_d)}\left[\mathcal{J}^\dagger_\mu\mathcal{J}^{\mu\dagger}\right]_i$$

$$\begin{aligned}&g_V^2(\boldsymbol{q}^2)\left(\bar{\psi}\gamma_\mu\tau_-\psi\right)^{(1)}\left(\bar{\psi}\gamma^\mu\tau_-\psi\right)^{(2)}, \\ &g_A^2(\boldsymbol{q}^2)\left(\bar{\psi}\gamma_\mu\gamma_5\tau_-\psi\right)^{(1)}\left(\bar{\psi}\gamma^\mu\gamma_5\tau_-\psi\right)^{(2)}, \\ &2g_A(\boldsymbol{q}^2)g_P(\boldsymbol{q}^2)\left(\bar{\psi}\boldsymbol{\gamma}\gamma_5\tau_-\psi\right)^{(1)}\left(\bar{\psi}\boldsymbol{q}\gamma_5\tau_-\psi\right)^{(2)}, \\ &g_P^2(\boldsymbol{q}^2)\left(\bar{\psi}\boldsymbol{q}\gamma_5\tau_-\psi\right)^{(1)}\left(\bar{\psi}\boldsymbol{q}\gamma_5\tau_-\psi\right)^{(2)}, \\ &g_M^2(\boldsymbol{q}^2)\left(\bar{\psi}\frac{\sigma_{\mu i}}{2m_p}q^i\tau_-\psi\right)^{(1)}\left(\bar{\psi}\frac{\sigma^{\mu j}}{2m_p}q_j\tau_-\psi\right)^{(2)}.\end{aligned}$$

L. S. Song et al., Phys. Rev. C 90, 054309 (2014).

Transition operator

- Relativistic form

$$\mathcal{H}_{\rm weak}(x) = \frac{G_F \cos\theta_C}{\sqrt{2}} j^\mu(x)\mathcal{J}^\dagger_\mu(x) + \text{h.c.},$$

$$\hat{\mathcal{O}}^{0\nu} = \sum_i \hat{\mathcal{O}}^{0\nu}_i, \quad (i = VV, AA, AP, PP, MM)$$

$$j^\mu($$

$$\mathcal{J}^\dagger_\mu(x)$$

$$- \quad g_A(q^2)\gamma_\mu\gamma_5 - g_P(q^2)q_\mu\gamma_5\big]\,\tau_-\psi(x),$$

$$M^{0\nu}(0^+_I \to 0^+_F) \equiv \langle 0^+_F|\hat{\mathcal{O}}^{0\nu}|0^+_I\rangle,$$

$$\frac{(\boldsymbol{x}_1-\boldsymbol{x}_2)}{+E_d)} \left[\mathcal{J}^\dagger_\mu \mathcal{J}^{\mu\dagger}\right]_i$$

$$)^{(2)},$$

$$g_A^2(\boldsymbol{q}^2)\left(\bar\psi\gamma_\mu\gamma_5\tau_-\psi\right)^{(1)}\left(\bar\psi\gamma^\mu\gamma_5\tau_-\psi\right)^{(2)},$$

$$2g_A(\boldsymbol{q}^2)g_P(\boldsymbol{q}^2)\left(\bar\psi\boldsymbol{\gamma}\gamma_5\tau_-\psi\right)^{(1)}\left(\bar\psi\boldsymbol{q}\gamma_5\tau_-\psi\right)^{(2)},$$

$$g_P^2(\boldsymbol{q}^2)\left(\bar\psi\boldsymbol{q}\gamma_5\tau_-\psi\right)^{(1)}\left(\bar\psi\boldsymbol{q}\gamma_5\tau_-\psi\right)^{(2)},$$

$$g_M^2(\boldsymbol{q}^2)\left(\bar\psi\frac{\sigma_{\mu i}}{2m_p}q^i\tau_-\psi\right)^{(1)}\left(\bar\psi\frac{\sigma^{\mu j}}{2m_p}q_j\tau_-\psi\right)^{(2)}.$$

Fully relativistic treatment:

L. S. Song et al., Phys. Rev. C 90, 054309 (2014).
J. M. Yao et al., Phys. Rev. C 91, 024316 (2015).

L. S. Song et al., Phys. Rev. C 90, 054309 (2014).

Transition operator

- Non-relativistic reduction

$$M^{0\nu}(0_I^+ \to 0_F^+) \equiv \langle 0_F^+ | \hat{\mathcal{O}}^{0\nu} | 0_I^+ \rangle,$$

$$\hat{\mathcal{O}}^{0\nu} = \sum_i \hat{\mathcal{O}}_i^{0\nu}, \quad (i = VV, AA, AP, PP, MM)$$

$$\hat{\mathcal{O}}_i^{0\nu} = \frac{4\pi R}{g_A^2} \int d^3x_1 d^3x_2 \int \frac{d^3q}{(2\pi)^3} \frac{\mathrm{e}^{\mathrm{i}\boldsymbol{q}\cdot(\boldsymbol{x}_1-\boldsymbol{x}_2)}}{q(q+E_d)} \left[\mathcal{J}_\mu^\dagger \mathcal{J}^{\mu\dagger}\right]_i$$

The non-relativistic "two-current" operator $\left[\mathcal{J}_\mu^\dagger \mathcal{J}^{\mu\dagger}\right]_{\mathrm{NR}}$ can be decomposed, as in other non-relativistic calculations, into the Fermi, the Gamow-Teller, and the tensor parts:

$$\left[-h_{\mathrm{F}}(\boldsymbol{q}^2) + h_{\mathrm{GT}}(\boldsymbol{q}^2)\sigma_{12} + h_{\mathrm{T}}(\boldsymbol{q}^2) S_{12}^q\right] \tau_-^{(1)} \tau_-^{(2)}, \quad (34)$$

with the tensor operator $S_{12}^q = 3(\boldsymbol{\sigma}^{(1)} \cdot \hat{\boldsymbol{q}})(\boldsymbol{\sigma}^{(2)} \cdot \hat{\boldsymbol{q}}) - \sigma_{12}$ and $\sigma_{12} = \boldsymbol{\sigma}^{(1)} \cdot \boldsymbol{\sigma}^{(2)}$. Each channel ($K$: F, GT, T) of Eq. (34) can be labeled by the terms of the hadronic current from which it originates, as

$$h_K(\boldsymbol{q}^2) = \sum_i h_{K-i}(\boldsymbol{q}^2), \quad (i = VV, AA, AP, PP, MM)$$

with

$$\begin{aligned}
h_{\mathrm{F}-VV}(\boldsymbol{q}^2) &= -g_V^2(\boldsymbol{q}^2), && (35a)\\
h_{\mathrm{GT}-AA}(\boldsymbol{q}^2) &= -g_A^2(\boldsymbol{q}^2), && (35b)\\
h_{\mathrm{GT}-AP}(\boldsymbol{q}^2) &= \frac{2}{3} g_A(\boldsymbol{q}^2) g_P(\boldsymbol{q}^2) \frac{\boldsymbol{q}^2}{2m_p}, && (35c)\\
h_{\mathrm{GT}-PP}(\boldsymbol{q}^2) &= -\frac{1}{3} g_P^2(\boldsymbol{q}^2) \frac{\boldsymbol{q}^4}{4m_p^2}, && (35d)\\
h_{\mathrm{GT}-MM}(\boldsymbol{q}^2) &= -\frac{2}{3} g_M^2(\boldsymbol{q}^2) \frac{\boldsymbol{q}^2}{4m_p^2}, && (35e)\\
h_{\mathrm{T}-AP}(\boldsymbol{q}^2) &= h_{GT-AP}(\boldsymbol{q}^2), && (35f)\\
h_{\mathrm{T}-PP}(\boldsymbol{q}^2) &= h_{GT-PP}(\boldsymbol{q}^2), && (35g)\\
h_{\mathrm{T}-MM}(\boldsymbol{q}^2) &= -\frac{1}{2} h_{GT-MM}(\boldsymbol{q}^2). && (35h)
\end{aligned}$$

F. Simkovic et. al, PRC 60, 055502 (1999)

L. S. Song et al., Phys. Rev. C 90, 054309 (2014).

Transition operator

- Non-relativistic

$$M^{0\nu}(0_I^+ \to 0_F^+$$

$$\hat{\mathcal{O}}^{0\nu} = \sum_i \hat{\mathcal{O}}_i^{0\nu}, \quad (i$$

$$\hat{\mathcal{O}}_i^{0\nu} = \frac{4\pi R}{g_A^2} \int d^3x_1 d^3$$

The non-relativistic "two-current" operator $\left[\mathcal{J}_\mu^\dagger \mathcal{J}^{\mu\dagger}\right]_{\rm NR}$ ativistic calcula-, and the tensor

$$\left.\right]\tau_-^{(1)}\tau_-^{(2)}, \quad (34)$$

$$\hat{q})(\boldsymbol{\sigma}^{(2)}\cdot\hat{\boldsymbol{q}}) - \sigma_{12}$$

$(K$: F, GT, T) of the hadronic

$$, AP, PP, MM)$$

(35a)

(35b)

$$q^2)\frac{\boldsymbol{q}^2}{2m_p}, \quad (35c)$$

$$\frac{}{}^2, \quad (35d)$$

$$\frac{}{}^2, \quad (35e)$$

$$, \quad (35f)$$

$$, \quad (35g)$$

$$\boldsymbol{q}^2). \quad (35h)$$

Table 1: The normalized NME $\tilde{M}^{0\nu}$ for the $0\nu\beta\beta$-decay obtained with the particle number projected spherical mean-field configuration ($\beta_I = \beta_F = 0$) by the PC-PK1 force using both the relativistic and non-relativistic reduced (first-order of q/m_p in the one-body current) transition operators. The ratio of the AA term to the total NME, $R_{AA} \equiv \tilde{M}^{0\nu}_{AA}/\tilde{M}^{0\nu}$, the relativistic effect $\Delta_{\rm Rel.} \equiv (\tilde{M}^{0\nu} - \tilde{M}^{0\nu}_{\rm NR})/\tilde{M}^{0\nu}$ and the ratio of the tensor part to the total NME, $R_T \equiv \tilde{M}^{0\nu}_{\rm NR,T}/\tilde{M}^{0\nu}_{\rm NR}$, are also presented.

Sph+PNP (PC-PK1)	$\tilde{M}^{0\nu}$	R_{AA}	$\tilde{M}^{0\nu}_{\rm NR}$	$\Delta_{\rm Rel.}$	R_T
^{48}Ca $\to$ ^{48}Ti	3.66	81%	3.74	−2.1%	−2.4%
^{76}Ge $\to$ ^{76}Se	7.59	94%	7.71	−1.6%	3.5%
^{82}Se $\to$ ^{82}Kr	7.58	93%	7.68	−1.4%	2.9%
^{96}Zr $\to$ ^{96}Mo	5.64	95%	5.63	0.2%	3.6%
^{100}Mo $\to$ ^{100}Ru	10.92	95%	10.91	0.1%	3.5%
^{116}Cd $\to$ ^{116}Sn	6.18	94%	6.13	0.7%	1.9%
^{124}Sn $\to$ ^{124}Te	6.66	94%	6.78	−1.8%	4.9%
^{130}Te $\to$ ^{130}Xe	9.50	94%	9.64	−1.4%	4.3%
^{136}Xe $\to$ ^{136}Ba	6.59	94%	6.70	−1.7%	4.1%
^{150}Nd $\to$ ^{150}Sm	13.25	95%	13.08	1.3%	2.5%

J. M. Yao et al., Phys. Rev. C 90, 054309 (2014)

F. Simkovic et. al, PRC 60, 055502 (1999) L. S. Song et al., Phys. Rev. C 90, 054309 (2014).

Transition operator

Neutrino potentials

Starting from the weak Lagrangian that describes the process some approximations are made:

1. Non-relativistic approach in the hadronic part.

2. Closure approximation in the virtual intermediate state.

3. Nucleon form factors taken in the dipolar approximation.

4. Tensor contribution is neglected.

5. High order currents are included (HOC).

6. Short range correlations are included with an UCOM correlator.

- Find the initial and final 0^+ (and, in the no closure approximation, the intermediate) states
- Evaluate the transition operators between these states

Transition operator

- The 'bare' operator should be transformed into an 'effective' operator defined in the valence space

MBPT

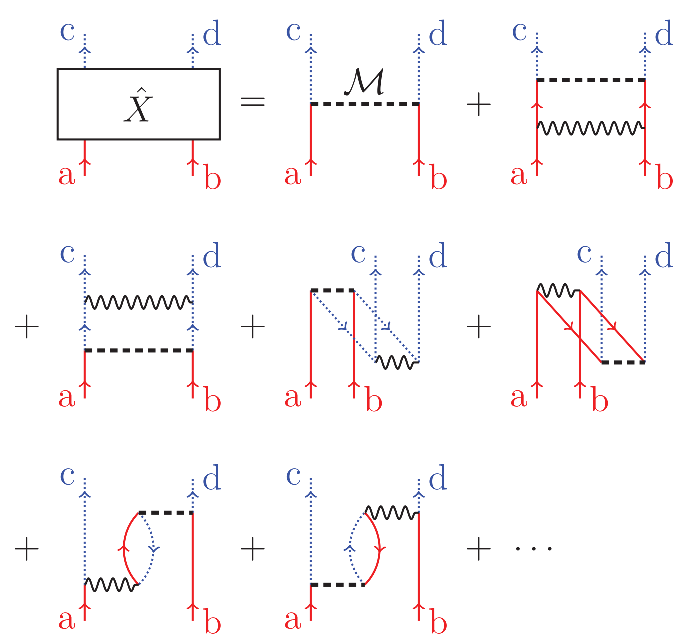

FIG. 2. (Color online) The $\hat{X}$ box to first order in $V_{\mathrm{low}\,k}$. Solid (red online) up- or down-going lines indicate neutrons and dotted (blue online) lines indicate protons. The wavy horizontal lines, as in Fig. 1, represent $V_{\mathrm{low}\,k}$, and the dashed horizontal lines represent the $0\nu\beta\beta$-decay operator in Eq. (1).

J.D. Holt, J. Engel, Phys. Rev. C 87, 064315 (2013)

Transition operator

- The ‘bare’ operator should be transformed into an ‘effective’ operator defined in the valence space

MBPT

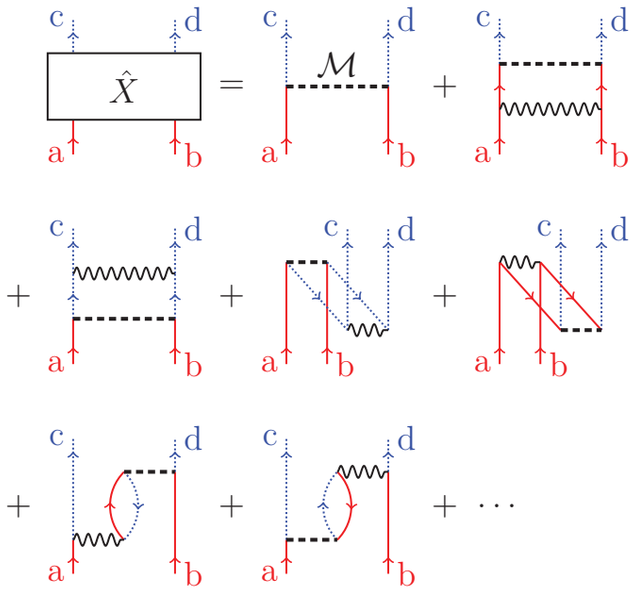

FIG. 2. (Color online) The $\hat{X}$ box to first order in $V_{\mathrm{low}\,k}$. Solid (red online) up- or down-going lines indicate neutrons and dotted (blue online) lines indicate protons. The wavy horizontal lines, as in Fig. 1, represent $V_{\mathrm{low}\,k}$, and the dashed horizontal lines represent the $0\nu\beta\beta$-decay operator in Eq. (1).

J.D. Holt, J. Engel, Phys. Rev. C 87, 064315 (2013)

- Two-body weak currents could play a relevant role

ISM

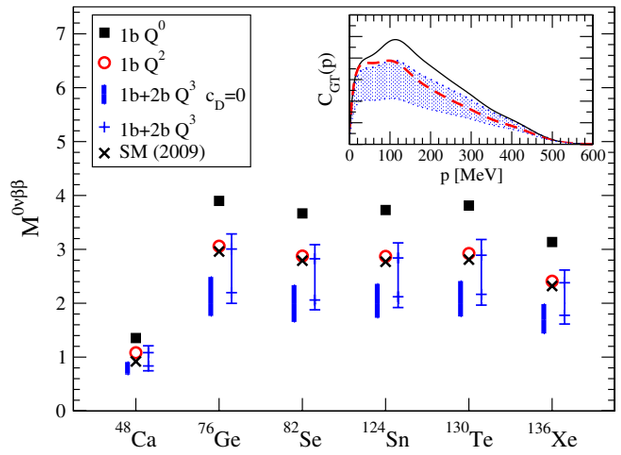

FIG. 2 (color online). Nuclear matrix elements $M^{0\nu\beta\beta}$ for $0\nu\beta\beta$ decay. At order Q^0, the NMEs include only the leading $p = 0$ axial and vector $1b$ currents. At the next order, all Q^2 $1b$-current contributions not suppressed by parity are taken into account. At order Q^3, the thick bars are predicted from the long-range parts of $2b$ currents ($c_D = 0$). The thin bars estimate the theoretical uncertainty from the short-range coupling c_D by taking an extreme range for the quenching (see text). For comparison, we show the SM results of Ref. [12] based on phenomenological $1b$ currents only. The inset (representative for ^{136}Xe) shows that the GT part, $M^{0\nu\beta\beta}_{\mathrm{GT}} = \int dp C_{\mathrm{GT}}(p)$, is dominated by $p \sim 100$ MeV.

J. Menéndez, D. Gazit, A. Schwenk, Phys. Rev. Lett. 107, 062501 (2011)

pnQRPA

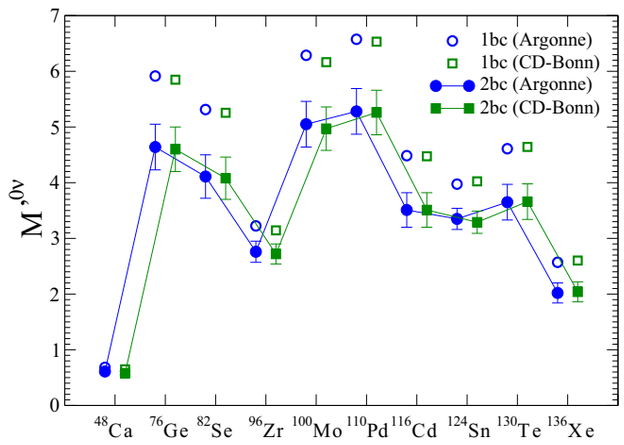

FIG. 1. (Color online) Nuclear matrix elements $M^{0\nu}$ for all the nuclei considered here. The empty circles and squares represent the results with the one-body current only, and the solid circles and squares the average of the results with two-body currents included. The error bars represent the dispersion in those values (see text).

J. Engel, F. Simkovic, P. Vogel, Phys. Rev. C 89, 064308 (2014)

Transition operator

- The 'bare' operator should be transformed into an 'effective' operator defined in the valence space

MBPT

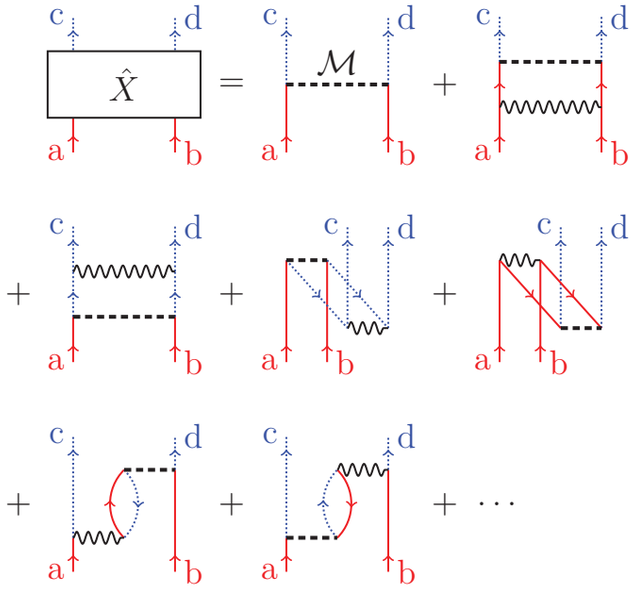

FIG. 2. (Color online) The $\hat{X}$ box to first order in $V_{\mathrm{low}\,k}$. Solid (red online) up- or down-going lines indicate neutrons and dotted (blue online) lines indicate protons. The wavy horizontal lines, as in Fig. 1, represent $V_{\mathrm{low}\,k}$, and the dashed horizontal lines represent the $0\nu\beta\beta$-decay operator in Eq. (1).

J.D. Holt, J. Engel, Phys. Rev. C 87, 064315 (2013)

- Two-body weak currents could play a relevant role

ISM

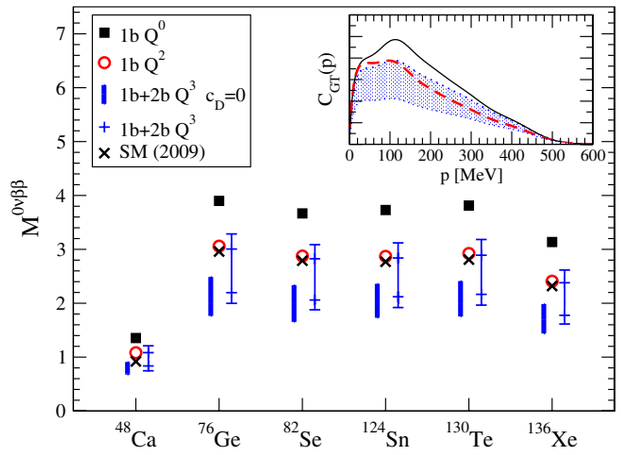

FIG. 2 (color online). Nuclear matrix elements $M^{0\nu\beta\beta}$ for $0\nu\beta\beta$ decay. At order Q^0, the NMEs include only the leading $p = 0$ axial and vector $1b$ currents. At the next order, all Q^2 $1b$-current contributions not suppressed by parity are taken into account. At order Q^3, the thick bars are predicted from the long-range parts of $2b$ currents ($c_D = 0$). The thin bars estimate the theoretical uncertainty from the short-range coupling c_D by taking an extreme range for the quenching (see text). For comparison, we show the SM results of Ref. [12] based on phenomenological $1b$ currents only. The inset (representative for ^{136}Xe) shows that the GT part, $M^{0\nu\beta\beta}_{\mathrm{GT}} = \int dp C_{\mathrm{GT}}(p)$, is dominated by $p \sim 100$ MeV.

J. Menéndez, D. Gazit, A. Schwenk, Phys. Rev. Lett. 107, 062501 (2011)

pnQRPA

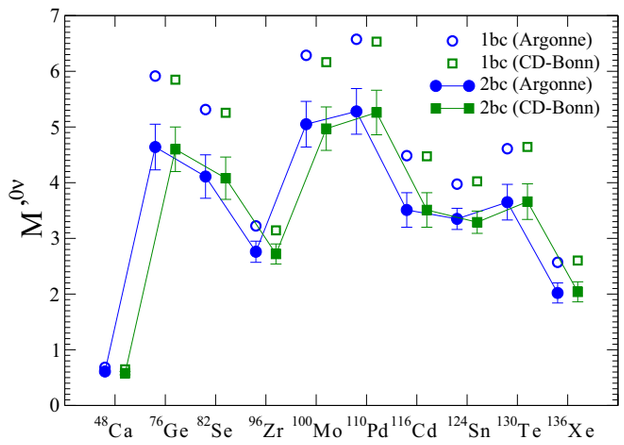

FIG. 1. (Color online) Nuclear matrix elements $M^{0\nu}$ for all the nuclei considered here. The empty circles and squares represent the results with the one-body current only, and the solid circles and squares the average of the results with two-body currents included. The error bars represent the dispersion in those values (see text).

J. Engel, F. Simkovic, P. Vogel, Phys. Rev. C 89, 064308 (2014)

➥ these are problems closely related to the quenching of Gamow-Teller strength

Open questions

- **Isospin mixing and restoration have to be done in the future. Why is it so difficult (perhaps impossible) with the current Gogny EDFs?**

- **Triaxiality has to be taken into account in *A*=76 and *A*=100 decays (at least).**

- **How relevant is the proper description of the spectra in 0νββ NMEs?**

- **Occupation numbers with EDF to define physically sound valence spaces.**

- **Odd-odd nuclei is still a major challenge for GCM calculations.**

- **Computational time?!?**